Population Modeling for Resource Allocation and Antimicrobial Stewardship

A Dissertation Presented for the

Doctor of Philosophy

Degree

The University of Tennessee, Knoxville

Jason Bintz

August 2015

I dedicate this dissertation to my wife and children. Your love is a miracle and a constant witness of the only credible ground of being.

Acknowledgements

I want to thank the University of Tennessee and, especially, the Department of Mathematics for giving me the opportunity to pursue a doctoral degree in mathematics. This was made possible through the generous financial support I received as a teaching assistant. I also want to thank the National Institute for Mathematical and Biological Synthesis (NIMBioS) for supporting me through a research assistantship and for the many other ways my education was enhanced by this affiliation.

I would like to thank the members of my committee, Judy Day, Yulong Xing, and Shigetoshi Eda. I am so grateful for your time and consideration of my work. I would also like to thank Cristina Lanzas for sharing her expertise, good advice and collaboration.

Preeminent thanks belong to my advisor, Suzanne Lenhart. Certainly, this dissertation would not have been possible apart from her constant support, patience and encouragement. Beyond that, and more importantly, in her I have an example that will continue to inspire me throughout my career.

Abstract

This dissertation contains two types of population models with applications in conservation biology and epidemiology. In particular, it considers models for resource allocation and antimicrobial stewardship.

In a population model with a parabolic differential equation and density dependent growth, we study the problem of allocating resources to maximize the net benefit in the conservation of a single species while the cost of the resource allocation is minimized. The net benefit is measured in terms of maximizing population abundance and the goal of maximizing abundance is divided between the goal of maximizing the overall abundance across space and time and the goal of maximizing abundance at the final time. We consider cases that model a fixed amount of resource as well as cases without this constraint. We regard the resource coefficient as a control and we consider cases where this coefficient varies in space and time as well as cases where it varies only in space. We establish the existence and uniqueness of the solution to the state system given a control and the existence of an optimal control. We establish the characterization of the optimal control and demonstrate uniqueness of the optimal control. Numerical simulations illustrate several cases with Dirichlet and Neumann boundary conditions.

We implement an agent-based model for *Clostridium difficile* transmission in hospitals that accounts for several processes and individual factors including environmental and antibiotic heterogeneity in order to evaluate the efficacy of various control measures aimed at reducing environmental contamination and mitigating the effects

of antibiotic use on transmission. In particular, we account for local contamination levels that contribute to the probability of colonization and we account for both the number and type of antibiotic treatments given to patients. Simulations illustrate the relative efficacy of several strategies for the reduction of nosocomial colonizations and nosocomial diseases.

Table of Contents

List of Tables

List of Figures

Chapter 1

Introduction

1.1 Optimal Control Theory

One of our goals in this work will be to determine the optimal growth coefficient for a population model that satisfies a certain objective. The context for this problem is the allocation of resources in conservation biology. Suppose that in an effort to conserve some species, you have resources at your disposal to allocate in some time horizon and across some habitat. What is the *best* way to do this? "Best" will involve some tradeoff between the *benefit* to the species and the associated *costs* of such allocation. This question has the two basic components of an optimal control problem, a state system dependent on some control and an objective functional. In this case the state system is a partial differential equation (PDE) that models the dynamics of a population and is influenced by a control variable that models the allocation of resources. Our objective functional models the goal of maximizing some benefit to the population while minimizing the associated cost of resource allocation.

Optimal control theory evolved from the calculus of variations. In the 1950's, L.S. Pontryagin and his collaborators developed the Maximum Principle for the optimal control of systems governed by ordinary differential equations (Pontryagin et al., 1962). A simple case of this type of optimal control problem is as follows.

Let control m belong to the set of admissible controls U. We seek $m^* \in U$ such that

$$J(m^*) = \max_{m \in U} J(m)$$

where

$$J(m) = \int_0^T f\left(t, x(t), m(t)\right)\, dt \tag{1.1.1}$$

subject to

$$\frac{d}{dt}x(t) = g\left(t, x(t), m(t)\right) \tag{1.1.2}$$

$$x(0) = x_0$$

where (1.1.1) is the objective functional, (1.1.2) is the state equation and x is called the state variable. If it exists, $m^*(t)$ is called an *optimal control*. We denote the corresponding state, $x^*(t)$, and together they form an *optimal pair*.

The key idea of Pontryagin was to append the state equation to the objective functional through the introduction of an adjoint variable. Using the adjoint function and differentiating J with respect to control u at u^* gives a characterization of the optimal control in terms of the state and adjoint functions. The coupled state-adjoint system together with the control characterization constitute the optimality system.

J.-L. Lions developed a general framework for analyzing optimal control problems with state systems governed by partial differential equations (Lions, 1971, 1972). While there is no full generalization of Pontryagin's Maximum Principle to optimal control of state systems governed by partial differential equations, some corresponding "maximum principle" type results can be found in Li and Yong (1995).

The setting for the problem of optimal control of PDEs is similar. Let control m belong to the set of admissible controls U. We seek $m^* \in U$ such that

$$J(m^*) = \sup_{m \in U} J(m),$$

subject to

$$Lu(x,t) = g(x,t,u(x,t),m(x,t))$$

with appropriate initial and boundary conditions. Here, L is a known partial differential operator and u is the state variable. We outline the solution technique employed in Chapter 2.

First, given a control, we establish the existence and uniqueness of the corresponding solution to the state system in an appropriate weak solution space. Then the existence of an optimal control is established. *A priori* estimates of the states in appropriate Sobolev spaces are needed for these results. Next, we derive necessary conditions for an optimal pair giving rise to an optimality system consisting of the coupled state-adjoint system and the characterization of the optimal control. Lastly, proving the existence and uniqueness of the solution to the optimality system implies the uniqueness of the optimal control.

1.2 Optimal Resource Allocation for a Parabolic Population Model

The effects of spatial heterogeneity on the dynamics of a population is an important issue in conservation biology. Motivated by the work of Cantrell and Cosner (Cantrell and Cosner, 1989, 1991b,a), we consider a population whose dynamics are subject to diffusion and density dependent, logistic growth. These dynamics are modeled by the PDE on a bounded domain

$$u(x,t)_t - \mu\Delta u(x,t) = u(x,t)\,(m - u(x,t)) \tag{1.2.1}$$

$$u(\cdot,0) = u_0 \tag{1.2.2}$$

with appropriate Neumann or Dirichlet boundary conditions and where $u = u(x,t)$ is the population density of a species at (x,t), $\mu > 0$ is the diffusion coefficient, m

is a growth coefficient related to the intrinsic growth rate of the population and the function u_0 is given.

One source of spatial heterogeneity is the spatio-temporal allocation of resources. Resource allocation can impact a population through its influence on the intrinsic growth rate of the species. We regard m, therefore, a control variable and in Chapter 2 we consider four control problems that we briefly describe here.

Let Ω be an open, connected, bounded subset of $\mathbb{R}^n$ with C^1 boundary $\partial\Omega$ and let $Q = \Omega \times (0, T)$ where $T \in (0, \infty)$. Define the control set, U_1 by

$$U_1 = \{m \in L^\infty(\Omega) : 0 \leq m(x) \leq M\}. \tag{1.2.3}$$

where M reflects the upper bound for the rate of resource allocation.

Alternatively, we consider the case where there is a fixed amount of resource to be allocated:

$$V_1 = \{m \in L^\infty(\Omega) : 0 \leq m(x) \leq M, \int_Q m(x)\, dxdt = \delta\}. \tag{1.2.4}$$

In each of these sets, the control is constant in time, $m = m(x)$.

We seek $m^* \in U_1$ or $m^* \in V_1$ such that

$$J(m^*) = \sup_m J(m)$$

where the objective functional, J_1, is defined by

$$J_1(m) = A \int_\Omega u(x, T)\, dx + \int_Q \left(u(x, t) - Bm(x)^2\right)\, dxdt. \tag{1.2.5}$$

and subject to (1.2.1) together with certain boundary and initial conditions. We will emphasize Neumann boundary conditions but will also compare results to problems with Dirichlet boundary conditions. Biologically, Neumann boundary

conditions represent a closed habitat whereas Dirichlet boundary conditions represent an inhospitable boundary.

The objective functional models the goal of maximizing population abundance while minimizing the quadratic costs associated with providing resources. The goal of maximizing abundance is divided between the goal of maximizing the overall abundance across space and time and the goal of maximizing abundance at the final time (payoff goal). Here A measures the relative importance of the population level at the final time, T, and B is a positive weight constant on the cost term.

We will also consider the case where m is a function of both space and time, $m = m(x,t)$. Define the control set U_2 by

$$U_2 = \{m \in L^\infty(Q) : 0 \leq m(x,t) \leq M\}. \tag{1.2.6}$$

For the case of a fixed amount of resource, we have the control set

$$V_2 = \{m \in L^\infty(Q) : 0 \leq m(x,t) \leq M, \int_Q m(x,t)\ dxdt = \delta\}. \tag{1.2.7}$$

We seek $m^* \in U_2$ or $m^* \in V_2$ such that

$$J_2(m^*) = \sup_m J_2(m)$$

where the objective functional, J_2, is defined by

$$J_2(m) = A\int_\Omega u(x,T)\,dx + \int_Q \left(u(x,t) - Bm(x,t)^2\right)\ dxdt, \tag{1.2.8}$$

subject to (1.2.1) and where A measures the relative importance of the population at time T compared with the population abundance over Q, and B is a positive weight constant on the cost term.

1.3 Antimicrobial Stewardship for the Control of *Clostridium difficile* Transmission in Health-care Settings

Clostridium difficile is an important hospital-acquired enteric pathogen. In particular, *Clostridium difficile* is the primary pathogen of antibiotic-associated colitis and accounts for up to 20% of antibiotic associated diarrhea in hospitals (Bartlett, 2002). The cost attributable to *Clostridium difficile* infection (CDI) in U.S. acute care facilities is estimated to be as much as $4.8 billion per year (Dubberke and Olsen, 2012).

CDI prevention measures have not changed sufficiently to manage these rising numbers. The focus of these measures is on testing symptomatic patients in order to identify patients with CDI so that isolation and contact precautions can be taken (Cohen et al., 2010; Dubberke et al., 2008). Recent studies, however, point out the significance to transmission within the ward of both transmission pathways beyond the ward itself and additional sources of CDI infections (Dubberke et al., 2014). Successful control measures will come only with a better understanding of *Clostridium difficile* transmission. In particular, there are three important sources of transmission heterogeneity that contribute to the incidence of CDI and, as such, successful control measures must take these into account.

One important source of transmission heterogeneity is environmental heterogeneity (Dubberke et al., 2008; Gerding et al., 2008). The risk of being colonized by *Clostridium difficile* varies significantly with local contamination levels (Dubberke et al., 2014). Control measures that address local contamination levels include contact precautions as well as cleaning and disinfection of the environment (Gerding et al., 2008).

Antibiotic treatments in hospitals provide another source of transmission heterogeneity. The CDI risk factors associated with antibiotics vary significantly by both

number of treatments and type of antibiotic (Slimings and Riley, 2014; Dancer et al., 2013). Antibiotic stewardship programs that reduce either the number of antibiotic treatments or the relative proportion of high risk antibiotic treatments are, therefore, important for the prevention and control of CDI (Feazel et al., 2014; Talpaert et al., 2011).

Finally, the role of asymptomatic carriers is a significant source of transmission heterogeneity. The admission of colonized, asymptomatic patients is significant to sustaining nosocomial transmission Lanzas et al. (2011). More effective control measures require a better understanding of transmission and, therefore, require a better understanding of the pre-admission history of patients with respect to factors pertinent to CDI and how these factors contribute to within-ward transmission.

The goal of this study is to evaluate the efficacy of various control measures aimed at reducing environmental contamination and mitigating the effects of antibiotic use on transmission for reducing the nosocomial incidence of colonization and infection. In Chapter 3 we, therefore, propose and implement an agent-based model for *Clostridium difficile* transmission in hospitals that accounts for these environmental, antibiotic, and patient heterogeneities.

Chapter 2

Optimal Resource Allocation for a Parabolic Population Model

2.1 Background

Understanding the effects of spatial heterogeneity in a habitat on population dynamics is an important issue in mathematical ecology (Kareiva et al., 1990; Tilman and Kareiva, 1997; Lou, 2006; Cantrell et al., 2009). Partial differential equations (PDEs) have long been used to model population dynamics (Murray, 2003; Holmes et al., 1994) and reaction-diffusion equations, in particular, have been studied extensively in spatial ecology (Okubo and Levin, 2001; Cantrell and Cosner, 2003). Skellam (1951) proposed the PDE on a bounded domain

$$u(x,t)_t - \mu\Delta u(x,t) = u(x,t)\left(m(x) - u(x,t)\right) \tag{2.1.1}$$

to describe the dynamics of a diffusing population that has density dependent, logistic growth. Here, $u(x,t)$ is the population density at (x,t), μ is the diffusion rate and $m(x)$ in the intrinsic growth rate of the population and can vary in space. Given an initial function, $u_0 = u(\cdot,0)$, a solution to (2.1.1) will also satisfy

appropriate boundary conditions such as no-flux (Neumann) or zero (Dirichlet) boundary conditions.

Cantrell and Cosner (1989) showed that the persistence of a population whose dynamics are modeled by (2.1.1), together with suitable boundary and initial conditions, depends on a relationship between the diffusion coefficient μ and $\lambda_1(m)$ where $\lambda_1(m)$ is the principal eigenvalue of the problem

$$-\Delta\phi = \lambda m(x)\phi.$$

In another study (Cantrell and Cosner, 1991b), they extended those results for a population model that included advection. In that case, persistence also depends on the advection coefficient. Other studies that include advection and pertain to persistence and are found in Belgacem and Cosner (1995); Cosner and Lou (2003); Cantrell et al. (2008).

In (Cantrell and Cosner, 1991a), they considered the arrangement within a habitat of "favorable" and "unfavorable" regions. Several such arrangements were considered and judged according to how severe were the constraints on population persistence. In particular, they considered steady states of (2.1.1) subject to Neumann, Dirichlet, or Robin boundary conditions and where $m = m(x)$ represents the intrinsic growth rate of the population u and can be considered to represent the resource function. In this work, Cantrell and Cosner considered the sign of $m(x)$ to indicate whether the habitat is favorable or unfavorable. To determine how suitable the overall habitat is for persistence, and following Murray and Sperb (1983), they considered the size of the principal eigenvalue of

$$-\Delta\phi = \lambda m(x)\phi.$$

As the size of this eigenvalue increases, the maximum rate of diffusion that will allow for persistence decreases.

Viewed from a slightly different perspective, one can think of the varying intrinsic growth rate as a response to the allocation of resources. The problem is now cast as

how should resources be allocated in order to benefit the population. In addition to its persistence, one may also consider the abundance of a population as in important metric for the effectiveness of conservation effort. Ding et al. (2010) addressed this question. In particular, they considered the following optimal control problem, using the intrinsic growth rate $m(x)$ as a control and the control set

$$U = \{m \in L^\infty(\Omega) \mid 0 \leq m(x) \leq M, \int_\Omega m(x)\, dx = \delta\},$$

where the integral constraint on m represents a fixed amount of resource to be allocated. They showed the existence of an optimal control, $m^* \in U$, such that

$$J(m^*) = \max_m J(m)$$

where the objective functional is

$$J(m) = \int_\Omega \Big[u - (Bm^2)\Big] dx,$$

subject to

$$\begin{aligned} -\mu\Delta u &= u(m-u) && \text{in} \quad \Omega \\ \frac{\partial u}{\partial \nu} &= 0 && \text{on} \quad \partial\Omega. \end{aligned}$$

Their objective functional sought to maximize the population level while minimizing the quadratic cost of control.

Optimal control theory evolved from the calculus of variations. In the 1950's, L.S. Pontryagin and his collaborators developed the Maximum Principle for the optimal control of systems governed by ordinary differential equations (Pontryagin et al., 1962). The key idea of Pontryagin was to append the state equation to the objective functional through the introduction of an adjoint variable. Using the adjoint function and differentiating J with respect to control m at m^* gives a characterization of the optimal control in terms of the state and adjoint functions. The coupled state-adjoint

system together with the control characterization constitute the optimality system. J.-L. Lions developed a general framework for analyzing optimal control problems with state systems governed by partial differential equations (Lions, 1971, 1972). While there is no full generalization of Pontryagin's Maximum Principle to optimal control of state systems governed by partial differential equations, some corresponding "maximum principle" type results can be found in Li and Yong (1995).

The studies just discussed concern steady state populations. There are, however, ecologically relevant contexts where the species being managed is not at a steady state. What spatio-temporal allocation of resources will maximize the population abundance while taking into account the costs associated with allocation? We address this question using the growth rate as a control in a parabolic PDE.

2.2 Problem Formulation

Let Ω be an open, connected, bounded subset of $\mathbb{R}^n$ with C^1 boundary $\partial\Omega$ and let $Q = \Omega \times (0,T)$ where $T \in (0,\infty)$. Let $u = u(x,t)$ be the population density of a species at $(x,t) \in Q$. We consider the problem:

$$\begin{aligned} u_t - \mu\Delta u &= u(m-u) \quad \text{in} \quad Q \\ u(\cdot,0) &= u_0 \quad \text{on} \quad \Omega \times \{t=0\}. \end{aligned} \tag{2.2.1}$$

Here $\mu > 0$ is the diffusion coefficient which is fixed. The function $m = m(x)$ or $m = m(x,t)$, is the "resource" function which is assumed to be bounded. The initial function $u_0 \in H^1(\Omega) \cap L^\infty(\Omega)$ is given and non-negative. We will emphasize Neumann boundary conditions

$$\frac{\partial u}{\partial \nu} = 0 \text{ on } \partial\Omega \times (0,T) \tag{2.2.2}$$

where ν is the outward normal vector on $\partial\Omega$, but will also compare results with Neumann boundary conditions to those with Dirichlet boundary conditions,

$$u = 0 \text{ on } \partial\Omega \times (0, T). \tag{2.2.3}$$

Biologically, Neumann boundary conditions represent a closed habitat for the species under management. For comparison, we also consider Dirichlet boundary conditions which means the population density is zero at the boundary due to a hostile area outside the boundary.

The goal is to maximize population abundance while minimizing the costs associated with providing resources. The goal of maximizing abundance is divided between the goal of maximizing the overall abundance across space and time and the goal of maximizing abundance at the final time (payoff goal). We formulate four control problems. Suppose the resource function varies only in space; i.e. $m = m(x)$. Our control set is given by

$$U_1 = \{m \in L^\infty(\Omega) : 0 \leq m(x) \leq M\}. \tag{2.2.4}$$

where M reflects the upper bound for the rate of resource allocation. Note that this upper bound imposes a limit on the total amount of resource that can be allocated.

Alternatively, we consider the case where there is a fixed amount of resource to be allocated across the entire space-time domain. This fixed amount is represented by the integral of m over Q:

$$V_1 = \{m \in L^\infty(\Omega) : 0 \leq m(x) \leq M, \int_Q m(x)\, dxdt = \delta\}. \tag{2.2.5}$$

In this case, we note the necessary relationship imposed on M and δ:

$$\delta = \int_Q m(x)\, dxdt \leq MT|\Omega|.$$

From a management perspective, if we require that all resources be allocated, then we must be able to allocate a sufficient amount at any given point in Q.

We seek $m^* \in U_1$ or $m^* \in V_1$ such that

$$J_1(m^*) = \sup_m J_1(m)$$

where the objective functional, J_1, is defined by

$$J_1(m) = A \int_\Omega u(x,T)\,dx + \int_Q \left(u(x,t) - Bm(x)^2\right)\,dxdt \tag{2.2.6}$$

and where A measures the relative importance of the population level at the final time, T, and B is a positive weight constant on the cost term. The objective functional models the goal described above to maximize population abundance (on $\Omega \times T$ and over Q) while minimizing the costs associated with providing resources.

We will also consider the case where m is a function of both space and time. Here our control set U_2 is given by

$$U_2 = \{m \in L^\infty(Q) : 0 \le m(x,t) \le M\}. \tag{2.2.7}$$

For the case of a fixed amount of resource, we have the control set

$$V_2 = \{m \in L^\infty(Q) : 0 \le m(x,t) \le M, \int_Q m(x,t)\,dxdt = \delta\} \tag{2.2.8}$$

and the necessary relationship imposed on M and δ is the same as before.

We seek $m^* \in U_2$ or $m^* \in V_2$ such that

$$J_2(m^*) = \sup_m J_2(m)$$

where the objective functional, J_2, is defined by

$$J_2(m) = A\int_\Omega u(x,T)\,dx + \int_Q \left(u(x,t) - Bm(x,t)^2\right)\,dxdt, \tag{2.2.9}$$

where A measures the relative importance of the population at time T compared with the population abundance over Q, and B is a positive weight constant on the cost term.

We consider our optimal control problems in appropriate weak solution spaces.

Weak Formulation for Neumann Boundary Conditions

The function $u \in V = L^2((0,T), H^1(\Omega)) \cap L^\infty(Q)$ with $u_t \in V^* = L^2((0,T), H^1(\Omega)^*)$ and $u(x,0) = u_0(x)$ is said to be a weak solution of (2.2.1) with Neumann boundary condition (2.2.2) if and only if

$$\int_0^T \langle u_t, \phi\rangle\,dt + \int_Q (\mu\nabla u)\cdot\nabla\phi\,dxdt = \int_Q u(m-u)\phi\,dxdt \tag{2.2.10}$$

for all $\phi \in L^2((0,T), H^1(\Omega))$, where the inner product $\langle\cdot,\cdot\rangle$ is the duality between $H^1(\Omega)^*$ and $H^1(\Omega)$. For Dirichlet boundary condition (2.2.3), the solution space is

$$u \in L^2((0,T), H_0^1(\Omega)) \cap L^\infty(Q) \text{ with } u_t \in L^2((0,T), H^{-1}(\Omega)).$$

2.3 *A priori* Estimates and Existence of Solutions

In this section, we state some preliminary results needed for proving the existence of and characterizing our optimal solutions. These results hold for both Dirichlet and Neumann boundary conditions. The first lemma states that all solutions u of PDE (2.2.1) must be positive.

Lemma 2.3.1. *Assume that $m \in V_2$ and $u_0 \in L^\infty(\Omega)$ and $u_0 \geq 0$. Then, any weak solution u of (2.2.1) with boundary condition (2.2.2) or (2.2.3) must be non-negative on Q.*

Proof. Consider the equation

$$u_t - \mu \Delta u = u(m - |u|). \tag{2.3.1}$$

Let $v(x,t) = \max\{-u(x,t), 0\}$. Using the weak form of (2.3.1), we have

$$\int_\Omega u_t v \, dx + \mu \int_\Omega \nabla u \cdot \nabla v \, dx = \int_\Omega uv(m - |u|) \, dx, \ t \in [0,T].$$

Consider the set $(x,t) \in Q$ such that $u(x,t) < 0$. On this set we have

$$u = -v; \quad u_t = -v_t; \quad \nabla u = -\nabla v; \quad v > 0.$$

Note that off this set, $v = 0$. Substitution yields

$$\begin{aligned} \frac{1}{2}\frac{d}{dt}\int_\Omega v^2 \, dx + \mu \int_\Omega |\nabla v|^2 \, dx &= \int_\Omega v^2(m - |u|) \, dx \\ &\leq \int_\Omega v^2 m \, dx \\ &\leq M \int_\Omega v^2 \, dx. \end{aligned}$$

This implies

$$\frac{d}{dt}\int_\Omega v^2 \, dx \leq 2M \int_\Omega v^2 \, dx$$

and Gronwall's inequality implies

$$\int_\Omega v^2 \, dx \leq e^{2MT} \int_\Omega v(x,0)^2 \, dx.$$

But $u_0(x) = u(x,0) \geq 0$ implies $v(x,0) = 0$. Thus, $\int_\Omega v^2 \, dx = 0, \forall t \in [0,T]$ and we have that $v = 0$ a.e. on Q, which gives $u \geq 0$ a.e. on Q. This being the case, PDE (2.3.1) is equivalent to PDE (2.2.1) and we have the result. □

The next lemma will be used to show our objective functional J_2 is bounded above.

Lemma 2.3.2. *Under the above assumptions and for each $m \in V_2$, any weak solution u of (2.2.1) with boundary condition (2.2.2) or (2.2.3) satisfies*

$$\int_\Omega u(x,t)dx \leq e^{Mt} \int_\Omega u_0(x)dx, \ \forall \ t \in [0,T].$$

where M is the upper bound on m. In particular, there exists a positive constant C such that

$$J_2(m) \leq C||u_0||_{L^\infty(\Omega)}, \quad \text{for all} \ \ m \in V_2.$$

Proof. Let $t \in [0,T]$. Assume a weak solution exists and let the test function $\phi = 1$. Since $u \geq 0$ by Lemma 2.3.1 and $m \leq M$, we have $um - u^2 \leq um \leq uM$ and thus

$$\int_\Omega u_t \, dx = \int_\Omega u(m-u) \, dx \leq M \int_\Omega u \, dx.$$

Applying Gronwall's inequality gives the first estimate and we have

$$\begin{aligned}
J_2(m) &= A \int_\Omega u(x,T)dx + \int_0^T \int_\Omega \left(u(x,t) - Bm(x,t)^2\right) \, dxdt \\
&\leq A \int_\Omega u(x,T)dx + \int_0^T \int_\Omega u(x,t) \, dxdt \\
&\leq Ae^{MT} \int_\Omega u_0(x) \, dx + \int_0^T e^{Mt} \int_\Omega u_0(x) \, dxdt \\
&= \left(Ae^{MT} + \int_0^T e^{Mt} \, dt\right) \int_\Omega u_0(x) \, dx \\
&= \left(Ae^{MT} + \frac{e^{MT}-1}{M}\right) \int_\Omega u_0(x) \, dx \\
&\leq \left(Ae^{MT} + \frac{e^{MT}-1}{M}\right) |\Omega| \cdot ||u_0||_{L^\infty}
\end{aligned}$$

□

The rest of the section is devoted to prove the existence and *a priori* estimates of the solutions u of the equation (2.2.1). Our first result is an energy estimate.

Lemma 2.3.3. *For every m in V_2, there exists a constant $C > 0$ depending on $\mu, |\Omega|$ and T such that the following estimate holds for any weak solution u of (2.2.1) with boundary conditions (2.2.2)*

$$||u||_{L^2(0,T;H^1(\Omega))} \leq C||u_0||_{L^2(\Omega)}.$$

Proof. It follows from Lemma 2.3.1 that $u \geq 0$. Thus, using the weak formulation with u as a test function, we get

$$\begin{aligned} \frac{1}{2}\frac{d}{dt}\int_\Omega u^2 dx + \mu \int_\Omega |\nabla u|^2 dx &= \int_\Omega (mu^2 - u^3) dx \\ &\leq M \int_\Omega u^2 dx \end{aligned} \tag{2.3.2}$$

where we used the upper bound on m and the non-negativity of u. This implies that there is a constant C_1 depending on the upper bound of our controls such that

$$\frac{d}{dt}\int_\Omega u(x,t)^2 dx + \mu \int_\Omega |\nabla u(x,t)|^2 dx \leq C_1 \int_\Omega u^2 dx. \tag{2.3.3}$$

Gronwall's inequality implies

$$\int_\Omega u(x,t)^2 dx \leq e^{C_1 T} \int_\Omega u_0(x)^2 dx = e^{C_1 T}||u_0||^2_{L^2(\Omega)} \quad \forall\ 0 \leq t < T. \tag{2.3.4}$$

Integrating (2.3.4) gives

$$\int_0^T \int_\Omega u(x,t)^2 dx dt \leq T e^{C_1 T}||u_0||^2_{L^2(\Omega)} \tag{2.3.5}$$

Integrating inequality (2.3.3) over $(0,T)$ gives

$$\int_0^T \frac{d}{dt}\int_\Omega u(x,t)^2 dxdt + \mu\int_0^T\int_\Omega |\nabla u(x,t)|^2 dxdt \leq C_1\int_0^T\int_\Omega u^2 dxdt$$

$$\int_\Omega u(x,T)^2 dx - \int_\Omega u(x,0)^2 dx + \mu\int_0^T\int_\Omega |\nabla u(x,t)|^2 dxdt \leq C_1\int_0^T\int_\Omega u^2 dxdt$$

$$\int_0^T\int_\Omega |\nabla u(x,t)|^2 dxdt \leq \frac{1}{\mu}\left(\int_\Omega u(x,0)^2 dx + C_1\int_0^T\int_\Omega u^2 dxdt\right)$$

This last estimate together with (2.3.5) yield

$$\begin{aligned}||u||^2_{L^2(0,T;H^1(\Omega))} &\leq Te^{C_1T}||u_0||^2_{L^2(\Omega)} + \frac{1}{\mu}\left(||u_0||^2_{L^2(\Omega)} + C_1Te^{C_1T}||u_0||^2_{L^2(\Omega)}\right)\\ &= \left(Te^{C_1T} + \frac{1+C_1Te^{C_1T}}{\mu}\right)||u_0||^2_{L^2(\Omega)}\end{aligned}$$

□

Next we estimate the time derivative u_t.

Lemma 2.3.4. *For every m in V_2, there exists a constant $C > 0$ such that the following estimate holds for any weak solution u of (2.2.1) with (2.2.2) and $||u||_{L^\infty(Q)} \leq C_1$*

$$||u_t||_{L^2(0,T;H^1(\Omega)^*)} \leq C$$

with C depending on $\mu, |\Omega|, ||u_0||_{L^\infty(\Omega)}, ||m||_{L^\infty(\Omega)}, T$ and C_1.

Proof. For each $\phi \in L^2(0,T,H^1(\Omega))$, the weak form of the solution u is

$$\begin{aligned}\int_0^T \langle u_t, \phi\rangle\, dt = -\mu\int_Q \nabla u\cdot\nabla\phi\, dxdt\\ + \int_Q mu\phi\, dxdt - \int_Q u^2\phi\, dxdt.\end{aligned}$$

Using the estimates for the states in $L^2(0,T,H^1(\Omega))$ we have

$$\left|\int_0^T \langle u_t,\phi\rangle\, dt\right| \leq C||\phi||_{L^2(0,T,H^1(\Omega))}$$

and thus

$$\|u_t\|_{L^2(0,T,H^1(\Omega)^*)} \leq C \tag{2.3.6}$$

with the constant C depending only on $\mu, |\Omega|, T, ||u_0||_{L^\infty}, ||m||_{L^\infty}$ and C_1. □

Now we construct the weak solution of our state PDE by an iteration method.

Theorem 2.3.5. *Let $0 < T < \infty$ and u_0 be non-negative, bounded in $H^1(\Omega) \cap L^\infty(\Omega)$. Then, for each $m \in V_2$, there is a unique weak solution u of (2.2.1) with (2.2.2). Moreover, there is a finite constant $C > 0$ depending only on $|\Omega|, \mu, T$, and $||u_0||_{L^\infty}$ such that*

$$0 \leq u(x,t) \leq C, \quad \forall\ (x,t) \in Q. \tag{2.3.7}$$

Proof. Consider the problem

$$\begin{aligned} U_t - \mu\Delta U &= mU && \text{in} && Q \\ \tfrac{\partial U}{\partial \nu} &= 0 && \text{on} && \partial\Omega \times (0,T) \\ U(x,\cdot) &= u_0(x) && \text{on} && \Omega \times \{t = 0\}. \end{aligned} \tag{2.3.8}$$

The function U is a supersolution of (2.2.1) with (2.2.2) and by a maximum principle for weak solutions of parabolic problems (Krylov, 1987) we have

$$0 \leq U(x,t) \leq ||u_0(x)||_{L^\infty(\Omega)} e^{MT}.$$

Let $u^1 = U$ and for $i = 2, 3, ...$ let u^i be the weak solution to

$$u^i_t - \mu\Delta u^i + Ru^i = Ru^{i-1} + u^{i-1}(m - u^{i-1}) \tag{2.3.9}$$

with initial condition $u_0(x)$ and boundary condition (2.2.2) where
$R > 2||u_0(x)||_{L^\infty(\Omega)} e^{MT}$.

These solutions exist since these PDEs are linear in u^i, given u^{i-1} (Evans, 2010).
Claim: For $i = 1, 2, ...$ we have

$$0 \leq u^i \leq U.$$

Clearly, $0 \leq u^1 \leq U$. Now suppose $0 \leq u^j \leq U$ for some $j > 1$. Then

$$\begin{aligned} u_t^{j+1} - \mu\Delta u^{j+1} + Ru^{j+1} &= Ru^j + u^j(m - u^j) \\ &= (R - (u^j - m))u^j \\ &\geq 0 \end{aligned}$$

since $u^j - m \leq u^j \leq U \leq ||u_0(x)||_{L^\infty(\Omega)} e^{MT} \leq R$. Thus by the maximum principle (Krylov, 1987), $u^{j+1} \geq 0$. By induction we have $0 \leq u^i$, for all $i \in \mathbb{N}$. Furthermore, since $u^1 = U$, we have

$$u_t^1 - \mu\Delta u^1 + Ru^1 = Ru^1 + mu^1.$$

Subtracting the u^{j+1} equation and using the induction hypothesis gives

$$\begin{aligned} (u^1 - u^{j+1})_t - \mu\Delta(u^1 - u^{j+1}) + R(u^1 - u^{j+1}) &= R(u^1 - u^j) + m(u^1 - u^j) + (u^j)^2 \\ &\geq 0. \end{aligned}$$

Now the maximum principle gives us $u^1 - u^{j+1} \geq 0$ which implies $u^{j+1} \leq U$. By induction we have $u^i \leq U$ for all $i \in \mathbb{N}$.

Next, we note that

$$\begin{aligned} \frac{\partial}{\partial u^{i-1}} \left(Ru^{i-1} + u^{i-1}(m - u^{i-1}) \right) &= R - (2u^{i-1} - m) \\ &> 0 \end{aligned}$$

since $2u^{i-1} - m \leq 2U \leq 2||u_0(x)||_{L^\infty(\Omega)} e^{MT} < R$. That is, the right-hand side of PDE (2.3.9) is increasing in u^{i-1}.

Claim: The state sequence is monotonically non-increasing:

$$u^{i+1} \leq u^i \qquad \forall i \in \mathbb{N}$$

Clearly $u^2 \leq u^1 = U$. Suppose $u^i \leq u^{i-1}$. Then

$$\begin{aligned}(u^i - u^{i+1})_t - \mu\Delta(u^i - u^{i+1}) + R(u^i - u^{i+1}) \\ &= \left(Ru^{i-1} + u^{i-1}(m - u^{i-1})\right) - \left(Ru^i + u^i(m - u^i)\right) \\ &\geq 0\end{aligned}$$

The result again follows by the maximum principle for weak solutions.

Note from the L^∞ bound on U, we obtain

$$||u^i||_{L^\infty(Q)} \leq C,$$

which is needed in the *a priori* estimates. By a similar argument as in Lemmas (2.3.3) and (2.3.4), we obtain similar *a priori* estimates for u^i. These estimates give us weak convergences *on a subsequence*. We need, however, convergence on the whole sequence due to the fact that PDE (2.3.9) involves u^i and u^{i-1}. The monotonic property established above gives us the weak convergences on the whole sequence. That is, there exists $u \in L^2(0, T, H^1(\Omega)) \cap L^\infty(Q)$ with $u_t \in L^2(0, T, H^1(\Omega)^*)$ such that

$$u^i \rightharpoonup u \in V \tag{2.3.10}$$

$$u^i_t \rightharpoonup u_t \in V^*. \tag{2.3.11}$$

Thus, in the weak form of (2.3.9) we have each of the terms on the left-hand side converging. For the right-hand side, we have

$$\lim_{i\to\infty} \int_Q u^{i-1} m\phi \, dxdt = \int_Q um\phi \, dxdt$$

since $m \in L^\infty(Q), \phi \in L^2(Q)$ implies $m\phi \in L^2(Q)$. For the last term we have the following

$$\begin{aligned}\left|\int_Q \left(u^i\right)^2 \phi \; dxdt - \int_Q u^2\phi \; dxdt\right| &= \left|\int_Q u^i(u^i - u)\phi \; dxdt + \int_Q u(u^i - u)\phi \; dxdt\right| \\ &\leq C\int_Q |u^i - u||\phi| \; dxdt \\ &\leq C\left(\int_Q |u^i - u|^2 \; dxdt\right)^{\frac{1}{2}}\left(\int_Q |\phi|^2 \; dxdt\right)^{\frac{1}{2}}.\end{aligned}$$

Because of monotonicity and weak convergence, a result of Simon (1987) gives us strong convergence,

$$u^i \to u \in L^2(Q),$$

and thus the right-hand side of the inequality goes to 0 as $i \to \infty$ and we have the desired convergence and that u satisfies PDE (2.2.10) with boundary condition (2.2.2).

For uniqueness, suppose u and v both satisfy (2.2.10). Using $u - v$ as a test function in each PDE, subtracting and using a similar technique as in the proof of Lemma (2.3.1) we have

$$\frac{d}{dt}\int_\Omega (u - v)^2 dx \leq C\int_\Omega (u - v)^2 dx. \tag{2.3.12}$$

Gronwall's inequality implies

$$\int_\Omega (u - v)^2 dx \leq e^{CT}\int_\Omega (u_0(x) - v_0(x))^2 dx \quad \forall t \in [0, T]. \tag{2.3.13}$$

Thus $u_0(x) = v_0(x)$ implies $u = v$. □

Remark: Theorem (2.3.5) also holds for controls in U_1, V_1, and U_2. Moreover, the results of this section are all valid for Dirichlet boundary conditions (2.2.3).

2.4 Existence of an Optimal Control

To investigate the maximum of our objective functional, we first show the existence of an optimal control.

Theorem 2.4.1. *Assume that $0 < T < \infty$, $u_0 \in L^\infty(\Omega) \cap H^1(\Omega)$ and u_0 is non-negative. There exists an optimal control $m^* \in V_2$ maximizing the objective functional $J_2(m)$, with states satisfying PDE (2.2.1) and boundary condition (2.2.2).*

Proof. By Lemma 2.3.2, $J_2(m) \leq C$ where C is a constant depending only on M, $||u_0||_{L^\infty(Q)}$ and T. Therefore, $\sup_{m\in V_2} J_2(m)$ exists. Let $\{m^n\}$ be a maximizing sequence in V_2, i.e.

$$\lim_{n\to\infty} J_2(m^n) = \sup_{m\in V_2} J_2(m). \tag{2.4.1}$$

Let $u^n = u(m^n)$ be the corresponding state solution when the control is m^n. We have shown *a priori* estimates for the states in $L^2((0,T), H^1(\Omega))$ and in $L^\infty(Q)$ and their time derivatives in $L^2((0,T), H^1(\Omega)^*)$.

By passing to a subsequence and using that $L^2(Q)$ is weakly compact, there exists u^* and m^* such that

$$u^n \rightharpoonup u^* \text{ in } L^2(0,T,H^1(\Omega)), \tag{2.4.2}$$

$$m^n \rightharpoonup m^* \text{ in } L^2(Q).$$

Since m^n is also in V_2, we have

$$\int_Q m^n dxdt = \delta.$$

Using the weak convergence in $L^2(Q)$ and test function $v = 1$ we have

$$\delta = \int_Q m^n \, dxdt \to \int_Q m^* \, dxdt.$$

That is, m^* is in V_2. Note that (2.3.7) implies u^* is in $L^\infty(Q)$.

Using the estimate on the time derivative from Lemma 2.3.4, Brézis (2010) and by passing to a subsequence, we have

$$\begin{aligned} u^n \to u^* \quad \text{in} \quad L^2(Q), \quad \nabla u^n \rightharpoonup \nabla u^* \quad \text{in} \quad L^2(Q), \quad \text{and} \\ u_t^n \rightharpoonup u_t^* \text{ in } L^2((0,T), H^1(\Omega)^*). \end{aligned} \tag{2.4.3}$$

We need to show that $u^* = u(m^*)$, meaning that u^* is the state corresponding to m^*, and that m^* is an optimal control.

From these convergences, it follows

$$\begin{aligned} &\lim_{n\to\infty} \int_Q u_t^n v \, dxdt = \int_Q u_t^* v \, dxdt, \\ &\lim_{n\to\infty} \int_Q (u^n)^2 \phi \, dxdt = \int_Q (u^*)^2 \phi \, dxdt. \\ &\lim_{n\to\infty} \int_Q \nabla u^n \cdot \nabla v \, dxdt = \int_Q \nabla u^* \cdot \nabla v \, dxdt. \end{aligned} \tag{2.4.4}$$

From the strong convergence of the sequence $\{u^n\}$ and the weak convergence of the sequence $\{m^n\}$, we obtain

$$\begin{aligned} &\Big| \int_Q m^n u^n \phi dxdt - \int_Q m^* u^* \phi \, dxdt \Big| \\ &= \Big| \int_Q m^n \phi (u^n - u^*) \, dxdt + \int_Q (m^n - m^*) \, \phi u^* \, dxdt \Big| \\ &\leq M \|\phi\|_{L^2(Q)} \|u^n - u^*\|_{L^2(Q)} + \Big| \int_Q (m^n - m^*) \phi u^* \, dxdt \Big| \\ &\to 0, \quad \text{as} \quad n \to \infty. \end{aligned}$$

using that $\phi u^* \in L^2(Q)$ due to $u^* \in L^\infty(Q)$.

Collecting the four convergence limits above, we pass to the limit in the four terms of our weak formulation of the PDEs for the u^n sequence and obtain $u^* = u(m^*)$.

Using the strong convergence in $L^2(Q)$ of the sequence u^n and the fact that the function $m \mapsto \int_Q |m|^2 dxdt$ is weakly lower semi-continuous in $L^2(Q)$ (Brézis, 2010),

we obtain

$$\sup_{m\in U} J(m) = \lim_{n\to\infty} J(m^n) = \int_Q [u^* - B|m^*|^2]dxdt = J(m^*).$$

We conclude that $m^* \in U$ is an optimal control. □

Remarks: A similar argument proves the case for control sets U_1, V_1, and U_2. The results of this section are all valid for Dirichlet boundary conditions (2.2.3).

2.5 Derivation of the Optimality System

The optimality system consists of the coupled state-adjoint system together with the characterization of the optimal control. We divide the characterizations into four cases for U_1, V_1, U_2 and V_2.

2.5.1 $U_1 = \{m \in L^\infty(\Omega) : 0 \le m(x) \le M\}$

We consider first the case where $m = m(x)$ and there is no specified amount of resource to allocate. To obtain the necessary conditions, we need to differentiate the map $m \mapsto J_1(m)$ with respect to the control m. We denote by $u = u(m)$ the unique, positive weak solution of PDE (2.2.1) with boundary condition (2.2.2). Since $u = u(m)$ appears in $J_1(m)$, we first prove the appropriate differentiability of the map $m \mapsto u(m)$ whose derivative is called the *sensitivity*.

Remark: Throughout this section we denote by ψ^ϵ the difference quotient

$$\psi^\epsilon = \frac{u(m+\epsilon l) - u(m)}{\epsilon}.$$

Theorem 2.5.1 (Sensitivity)**.** *The mapping $m \in U_1 \mapsto u(m) \in V$ is differentiable in the following sense: for each m, l in U_1 such that $m + \epsilon l \in U_1$ for all ϵ sufficiently*

small, then there exist $\psi \in V$ *and* $\psi_t \in V^*$ *such that*

$$\psi^\epsilon \rightharpoonup \psi \text{ weakly in } V \text{ as } \epsilon \to 0, \tag{2.5.1}$$

$$(\psi^\epsilon)_t \rightharpoonup (\psi)_t \text{ weakly in } V^* \text{ as } \epsilon \to 0, \tag{2.5.2}$$

and the sensitivity ψ *satisfies*

$$\begin{array}{rcll} \psi_t - \mu\Delta\psi - (m-2u)\psi & = & ul & \text{in } Q, \\ \dfrac{\partial\psi}{\partial\nu} & = & 0 & \text{on } \partial\Omega \times (0,T), \\ \psi & = & 0 & \text{on } \Omega \times \{t=0\}. \end{array} \tag{2.5.3}$$

Proof. Let $u^\epsilon = u(m^\epsilon)$ where $m^\epsilon = m + \epsilon\ell$. The state PDEs corresponding to controls m^ϵ and m are given by

$$u_t^\epsilon - \mu\Delta u^\epsilon = u^\epsilon (m^\epsilon - u^\epsilon) \tag{2.5.4}$$

$$u_t - \mu\Delta u = u(m-u). \tag{2.5.5}$$

Taking differences and dividing by ϵ we have:

$$\left(\frac{u^\epsilon - u}{\epsilon}\right)_t - \mu\Delta\left(\frac{u^\epsilon - u}{\epsilon}\right) = \frac{u^\epsilon m^\epsilon - um}{\epsilon} - \frac{(u^\epsilon)^2 - u^2}{\epsilon} \tag{2.5.6}$$

$$= \left(\frac{u^\epsilon - u}{\epsilon}\right) m + u^\epsilon \ell - \frac{u^\epsilon - u}{\epsilon}(u^\epsilon + u). \tag{2.5.7}$$

The PDE satisfied by the difference quotient is given by

$$\psi_t^\epsilon - \mu\Delta\psi^\epsilon = (m - (u^\epsilon + u))\psi^\epsilon + u^\epsilon \ell \tag{2.5.8}$$

A priori estimates on the quotients ψ^ϵ can be shown similarly to the estimates on the states:

$$||\psi^\epsilon||_V \leq C_1$$

$$||\psi_t^\epsilon||_{V^*} \leq C_2.$$

Thus there exists $\psi \in V$ with $\psi_t \in V^*$ that is the weak limit of ψ^ϵ as in (2.5.1) and (2.5.2). Note that we also obtain $u^\epsilon \to u$ in V by $||u^\epsilon - u||_V \leq \epsilon C_1$. This gives convergence of the $u^\epsilon \ell$ and $u^\epsilon \psi^\epsilon$ terms. By these convergences, the sensitivity ψ satisfies the desired PDE. Similarly, the sensitivity PDE satisfies the given boundary and initial conditions. □

Next, we characterize our optimal control solution m^* by differentiating the map $m \mapsto J_1(m)$. We use the sensitivity equation to find our adjoint equation and our characterization. The sensitivity PDE can be rewritten as $L\psi = u\ell$ where

$$L\psi = \left(\frac{\partial}{\partial t} - \mu\Delta - (m - 2u)\right)\psi.$$

In order to introduce the sensitivity PDE into our objective functional, we make use of an adjoint PDE. The formal adjoint of the operator L is the operator L^* satisfying:

$$\langle p, L\psi\rangle = \langle L^* p, \psi\rangle$$

in an L^2 sense.

To see the specific terms, we integrate (formally) by parts:

$$\int_Q pL\psi \; dxdt = \int_Q p\left(\psi_t - \mu\Delta\psi - (m-2u)\psi\right) \; dxdt \tag{2.5.9}$$

$$= \int_Q p\psi_t \; dxdt - \mu\int_Q p\Delta\psi \; dxdt - \int_Q p(m-2u)\psi \; dxdt \tag{2.5.10}$$

$$= -\int_Q p_t\psi \; dxdt + \int_\Omega p(x,T)\psi(x,T) \; dx - \int_\Omega p(x,0)\psi(x,0) \; dx \tag{2.5.11}$$

$$+ \mu\int_Q \nabla p\nabla\psi \; dxdt - \mu\int_0^T\int_{\partial\Omega} p\frac{\partial\psi}{\partial\nu} \; dSdt \tag{2.5.12}$$

$$- \int_Q p(m-2u)\psi \; dxdt \tag{2.5.13}$$

$$= -\int_Q p_t\psi dxdt + \int_\Omega p(x,T)\psi(x,T)dx - \int_\Omega p(x,0)\psi(x,0)dx \tag{2.5.14}$$

$$- \mu\int_Q \psi\Delta p \; dxdt + \mu\int_0^T\int_{\partial\Omega} \psi\frac{\partial p}{\partial\nu} \; dSdt \tag{2.5.15}$$

$$- \mu\int_0^T\int_{\partial\Omega} p\frac{\partial\psi}{\partial\nu} \; dSdt - \int_Q p(m-2u)\psi \; dxdt. \tag{2.5.16}$$

The boundary and initial conditions of the sensitivity PDE (2.5.3) give:

$$\int_Q pL\psi \; dxdt = \int_Q \left(-p_t - \mu\Delta p - p(m-2u)\right)\psi \; dxdt \tag{2.5.17}$$

$$+ \int_\Omega p(x,T)\psi(x,T) \; dx + \mu\int_0^T\int_{\partial\Omega} \psi\frac{\partial p}{\partial\nu} \; dSdt \tag{2.5.18}$$

$$= \int_Q \psi L^*p \; dxdt + \int_\Omega p(x,T)\psi(x,T) \; dx \tag{2.5.19}$$

$$+ \mu\int_0^T\int_{\partial\Omega} \psi\frac{\partial p}{\partial\nu} \; dSdt. \tag{2.5.20}$$

When we take the derivative (with respect to the control) of the terms in the integrand of the objective functional that involve the state, we will have

$$\frac{\partial \text{ integrand of } J_1}{\partial \text{ state}} \cdot \frac{\partial \text{ state}}{\partial \text{ control}} = 1 \cdot \psi$$

This suggests how to define the right hand side (RHS) of the adjoint PDE. Namely, the RHS of the adjoint PDE should be the derivative of the integrand with respect to the state. The basic idea can be illustrated in this way:

$$\frac{\partial \text{ integrand of } J_1}{\partial \text{ state}} \cdot \frac{\partial \text{ state}}{\partial \text{ control}} = \text{Adjoint}_{RHS} \cdot \psi = \psi L^* p = pL\psi = p \cdot \text{State}_{RHS}$$

Moreover, since J_1 has a term involving the state at the final time (payoff term), a similar line of reasoning suggests how to define the final time condition for the adjoint PDE; i.e. $p = A$ at $t = T$.

Theorem 2.5.2. *Given an optimal control $m^* \in U_1$ and corresponding state $u^* = u(m^*)$, there exists an adjoint p in $L^2(0,T,H^1(\Omega)) \cap L^\infty(Q)$ which satisfies $p_t \in L^2((0,T),H^1(\Omega)^*)$ and*

$$\begin{aligned} -p_t - \mu\Delta p - (m^* - 2u^*)p &= 1 \quad \text{in } Q, \\ \frac{\partial p}{\partial \nu} &= 0 \quad \text{on } \partial\Omega \times (0,T), \\ p &= A \quad \text{on } \Omega \times \{t = T\}. \end{aligned} \tag{2.5.21}$$

Furthermore, m^* is characterized by

$$m^*(x) = \min\left\{M, \max\left\{\frac{\int_0^T (u^* p)(x,t)dt}{2BT}, 0\right\}\right\} \tag{2.5.22}$$

Proof. Suppose m^* is an optimal control. Let $l \in U_1$ such that $m^* + \epsilon l \in U_1$ for sufficiently small $\epsilon > 0$. Let $u^\epsilon = u(m^* + \epsilon l)$ denote the unique solution of (2.2.1) when the control term is $m^* + \epsilon l$.

Problem (2.5.21) is linear in p and its coefficients are measurable and bounded. By the change of variable $t \to T - t$, the existence and uniqueness of the weak solution p of (2.5.21) follows by Galerkin's method (Evans, 2010).

Now, observe that the directional derivative of J_1 with respect to the control at m^* in the direction of l satisfies

$$\begin{aligned}
0 &\geq \lim_{\epsilon \to 0^+} \frac{J_1(m^* + \epsilon l) - J_1(m^*)}{\epsilon} \\
&= \lim_{\epsilon \to 0^+} A \int_\Omega \frac{(u^\epsilon - u^*)}{\epsilon}(x,T)\ dx \\
&\qquad + \lim_{\epsilon \to 0^+} \int_Q \left(\frac{(u^\epsilon - u^*)}{\epsilon}(x,t) - B\frac{(m^* + \epsilon l)(x)^2 - m^*(x)^2}{\epsilon} \right) dxdt \\
&= A \int_\Omega \psi(x,T)\ dx + \int_Q (\psi(x,t) - 2Bm^*(x)l(x))\, dxdt.
\end{aligned}$$

Using the weak solution formulation for the adjoint problem with test function ψ, we obtain

$$\begin{aligned}
0 &\geq A \int_\Omega \psi(x,T)\ dx + \int_Q \psi(x,t)\ dxdt - \int_0^T \int_\Omega 2Bm^*(x)l(x)\ dxdt \\
&= \int_\Omega A\psi(x,T)\ dx + \int_Q ((-p_t - (m^* - 2u^*)p)\psi + \mu \nabla p \cdot \nabla \psi)\ \ dxdt \\
&\qquad\qquad - T \int_\Omega 2Bm^*(x)l(x)\ dx \\
&= \int_Q ((\psi_t - (m^* - 2u^*)\psi)p + \mu \nabla p \cdot \nabla \psi)\ \ dxdt - T \int_\Omega 2Bm^*(x)l(x)\ dx \\
&= \int_Q pu^*(x,t)l(x)\ dxdt - T \int_\Omega 2Bm^*(x)l(x)\ dx \\
&= \int_\Omega l(x) \left(-2BTm^*(x) + \int_0^T (u^*p)(x,t)\ dt \right)\ dx.
\end{aligned} \tag{2.5.23}$$

The sensitivity PDE was used to simplify this calculation.

Consider variation l with support on the set $0 < m^* < M$. Since m^* is on the interior of the control set, l can have arbitrary sign. Thus, on this set we have

$$-2BTm^*(x) + \int_0^T (u^*p)(x,t)\ dt = 0$$

which implies

$$m^*(x) = \frac{\int_0^T u^*p(x,t)dt}{2BT}.$$

On the set where $m^* = 0$ and l has support, $l \geq 0$ and we have

$$m^*(x) = 0 \geq \frac{\int_0^T u^* p(x,t) dt}{2BT}.$$

Finally, on the set where $m^* = M$ and l has support, $l \leq 0$ and we have

$$m^*(x) = M \leq \frac{\int_0^T u^* p(x,t) dt}{2BT}.$$

Putting these cases together gives the desired control characterization. □

2.5.2 $V_1 = \{m \in L^\infty(\Omega) : 0 \leq m(x) \leq M, \int_Q m(x)\ dxdt = \delta\}$

To obtain a control characterization for the case with a fixed amount of resources, we introduce a new state variable, w in $H^1(\Omega)$ satisfying

$$\begin{array}{rcll} \Delta w & = & m & \text{in } \Omega \\ \dfrac{\partial w}{\partial \nu} & = & \dfrac{\delta}{T|\partial\Omega|} & \text{on } \partial\Omega. \end{array} \tag{2.5.24}$$

A weak solution to (2.5.24) exists (Evans, 2010). To see how this satisfies the desired constraint, we integrate m over Ω, substitute the Laplacian of the new state and integrate by parts:

$$\begin{aligned} \int_Q m(x)\ dxdt &= T \int_\Omega m(x)\ dx \\ &= T \int_\Omega \Delta w\ dx \\ &= T \int_{\partial\Omega} \nabla w \cdot \nu\ dSdx \\ &= T \int_{\partial\Omega} \frac{\partial w}{\partial \nu}\ dSdx \\ &= \delta. \end{aligned}$$

Remark: Consider the case $n = 1$ with $\Omega = (0, 1)$. Using the discrete measure, $|\partial\Omega| = 2$, and we have

$$\begin{aligned} w''(x) &= m(x) \quad \text{in} \quad (0,1) \\ w'(0) \cdot (-1) &= \tfrac{\delta}{2T} \\ w'(1) \cdot (1) &= \tfrac{\delta}{2T} \end{aligned}$$

which gives the following:

$$\begin{aligned} \int_0^T \int_0^1 m(x)\, dxdt &= T \int_0^1 m(x)\, dx \\ &= T \int_0^1 w''(x)\, dx \\ &= T \left(w'(x) \Big|_0^1 \right) \\ &= T \left(w'(1) - w'(0) \right) \\ &= T \left(\frac{\delta}{2T} - \frac{-\delta}{2T} \right) \\ &= \delta. \end{aligned}$$

The problem of maximizing J_1 (2.2.6) over V_1 (2.2.5) is now recast as that of maximizing J_1 (2.2.6) over U_1 (2.2.4) such that a corresponding pair (u, w) exists satisfying (2.2.1) together with boundary condition (2.2.2) and (2.5.24) respectively. Now we will have a system of two sensitivities, ψ_1 and ψ_2.

Theorem 2.5.3 (Sensitivity)**.** *The mapping $m \in U_1 \mapsto (u, w)(m)$ is differentiable in the following sense: for each m, l in U_1 such that $m + \epsilon l \in U_1$ for all ϵ sufficiently small, then there exist $\psi_1 \in V, (\psi_1)_t \in V^*$ and $\psi_2 \in H^1(\Omega)$, such that*

$$\psi_1^\epsilon \rightharpoonup \psi_1 \text{ weakly in } V \text{ as } \epsilon \to 0, \tag{2.5.25}$$

$$(\psi_1^\epsilon)_t \rightharpoonup (\psi_1)_t \text{ weakly in } V^* \text{ as } \epsilon \to 0, \tag{2.5.26}$$

$$\psi_2^\epsilon \rightharpoonup \psi_2 \text{ weakly in } H^1(\Omega) \text{ as } \epsilon \to 0, \tag{2.5.27}$$

and the sensitivities ψ_1 and ψ_2 satisfy

$$\begin{aligned} \psi_{1t} - \mu\Delta\psi_1 - (m-2u)\psi_1 &= ul \quad \text{in } Q, \\ \frac{\partial\psi_1}{\partial\nu} &= 0 \quad \text{on } \partial\Omega \times (0,T), \\ \psi_1 &= 0 \quad \text{on } \Omega \times \{t=0\}. \end{aligned} \tag{2.5.28}$$

$$\begin{aligned} \Delta\psi_2 &= l \quad \text{in } \Omega, \\ \frac{\partial\psi_2}{\partial\nu} &= 0 \quad \text{on } \partial\Omega. \end{aligned} \tag{2.5.29}$$

Proof. A priori estimates on the quotients ψ_1^ϵ and ψ_2^ϵ can be shown similarly to the estimates on the states:

$$||\psi_1^\epsilon||_V \leq C_1$$

$$||(\psi_1^\epsilon)_t||_{V^*} \leq C_2.$$

$$||\psi_2^\epsilon||_V \leq C_3$$

Thus there exist $\psi_1 \in V$ with $(\psi_1)_t \in V^*$ and $\psi_2 \in H^1(\Omega)$ that are the weak limits of ψ_1^ϵ and ψ_2^ϵ as in (2.5.25), (2.5.26), and (2.5.27).

That sensitivity ψ_1 satisfies (2.5.28) was shown in Theorem 2.5.1. Let $w^\epsilon = w\left(m^\epsilon\right)$ where $m^\epsilon = m + \epsilon\ell$. The state PDEs corresponding to controls m^ϵ and m are given by

$$\Delta w^\epsilon = m^\epsilon \tag{2.5.30}$$

$$\Delta w = m \tag{2.5.31}$$

Taking differences and dividing by ϵ we have:

$$\Delta\left(\frac{w^\epsilon - w}{\epsilon}\right) = \ell \tag{2.5.32}$$

That is, the PDE satisfied by the difference quotient is given by

$$\Delta\psi_2^\epsilon = \ell \tag{2.5.33}$$

Note that ψ_2^ϵ doesn't depend on epsilon and the sensitivity ψ_2 satisfies the desired PDE. Similarly, the sensitivity satisfies the given boundary conditions. □

Theorem 2.5.4. *Given an optimal control m^* in V_1 and corresponding state (u^*, w^*), there exists (p_1, p_2) with $p_1 \in L^2(0,T,H^1(\Omega)) \cap L^\infty(Q), p_{1_t} \in L^2((0,T), H^1(\Omega)^*)$, and $p_2 \in H^1(\Omega)$ satisfying*

$$\begin{aligned} -p_{1_t} - \mu\Delta p_1 - (m^* - 2u^*)p_1 &= 1 \quad \text{in } Q, \\ \frac{\partial p_1}{\partial \nu} &= 0 \quad \text{on } \partial\Omega \times (0,T), \\ p_1 &= A \quad \text{on } \Omega \times \{t = T\}. \end{aligned} \tag{2.5.34}$$

$$\begin{aligned} \Delta p_2 &= 0 \quad \text{in } \Omega, \\ \frac{\partial p_2}{\partial \nu} &= 0 \quad \text{on } \partial\Omega. \end{aligned} \tag{2.5.35}$$

Furthermore, m^* is characterized by

$$m^*(x) = \min\left\{M, \max\left\{\frac{p_2(x) + \int_0^T (u^* p_1)(x,t)dt}{2BT}, 0\right\}\right\} \tag{2.5.36}$$

Proof. The proof follows just as with Theorem 2.5.2 except that inequality (2.5.23) picks up an extra term for the new state:

$$\begin{aligned}
0 &\geq A\int_\Omega \psi_1(x,T)\ dx + \int_Q \psi_1\ dxdt - T\int_\Omega 2Bm^*l\ dx \\
&= A\int_\Omega \psi_1(x,T)\ dx + \int_Q \left((-(p_1)_t - (m^*-2u^*)p_1)\psi_1 + \mu\nabla p_1\cdot\nabla\psi_1\right)\ dxdt \\
&\qquad - T\int_\Omega 2Bm^*l\ dx - \int_\Omega \nabla p_2\cdot\nabla\psi_2\ dx \\
&= \int_Q \left(((\psi_1)_t - (m^*-2u^*)\psi_1)p_1 + \mu\nabla p_1\cdot\nabla\psi_1\right)\ dxdt \\
&\qquad - T\int_\Omega 2Bm^*l\ dx + \int_\Omega p_2 l\ dx \\
&= \int_Q l(x)(u^*p_1)(x,t)\ dxdt - \int_\Omega l(x)\left(2BTm^*(x) - p_2(x)\right)\ dx \\
&= \int_\Omega l(x)\left(-2BTm^*(x) + p_2(x) + \int_0^T (u^*p_1)(x,t)\ dt\right)\ dx.
\end{aligned} \tag{2.5.37}$$

Again, by taking cases on the sets where $0 < m^* < M$, $m^* = M$, and $m^* = 0$, one obtains the desired control characterization. □

Remark: The solution p_2 to (2.5.35) is a constant chosen in such a way that the integral constraint on m is satisfied.

2.5.3 $U_2 = \{m \in L^\infty(Q) : 0 \leq m(x,t) \leq M\}$

We now consider our control as a function of both space and time. In order to characterize the optimal control, we need to differentiate the maps $m \mapsto J_2(m)$ and $m \mapsto u(m)$ with respect to the control m.

Theorem 2.5.5 (Sensitivity)**.** *The mapping $m \in U_2 \mapsto u(m) \in V$ is differentiable in the following sense: for each m, l in U_2 such that $m + \epsilon l \in U_2$ for all ϵ sufficiently*

small, then there exist $\psi \in V$ *and* $\psi_t \in V^*$ *such that*

$$\psi^\epsilon \rightharpoonup \psi \text{ weakly in } V \text{ as } \epsilon \to 0, \tag{2.5.38}$$

$$(\psi^\epsilon)_t \rightharpoonup (\psi)_t \text{ weakly in } V^* \text{ as } \epsilon \to 0, \tag{2.5.39}$$

and the sensitivity ψ *satisfies*

$$\begin{aligned} \psi_t - \mu\Delta\psi - (m - 2u)\psi &= ul \quad \text{in } Q, \\ \frac{\partial\psi}{\partial\nu} &= 0 \quad \text{on } \partial\Omega \times (0,T), \\ \psi &= 0 \quad \text{on } \Omega \times \{t = 0\}. \end{aligned} \tag{2.5.40}$$

Proof. The proof is similar to the proof of Theorem 2.5.1. □

Next we use the adjoint function for our control characterization.

Theorem 2.5.6. *Given an optimal control* $m^* \in U_2$ *and corresponding state* $u^* = u(m^*)$*, there exists an adjoint* p *in* $L^2(0,T,H^1(\Omega)) \cap L^\infty(Q)$ *which satisfies* $p_t \in L^2((0,T),H^1(\Omega)^*)$ *and*

$$\begin{aligned} -p_t - \mu\Delta p - (m^* - 2u^*)p &= 1 \quad \text{in } Q, \\ \frac{\partial p}{\partial\nu} &= 0 \quad \text{on } \partial\Omega \times (0,T), \\ p &= A \quad \text{on } \Omega \times \{t = T\}. \end{aligned} \tag{2.5.41}$$

Furthermore, m^* *is characterized by*

$$m^*(x,t) = \min\left\{M, \max\left\{\frac{(u^*p)(x,t)}{2B}, 0\right\}\right\} \tag{2.5.42}$$

Proof. The directional derivative of J_2 with respect to the control at m^* in the direction of l satisfies

$$\begin{aligned}
0 &\geq \lim_{\epsilon \to 0^+} \frac{J_2(m^* + \epsilon l) - J_2(m^*)}{\epsilon} \\
&= \lim_{\epsilon \to 0^+} \left(A \int_\Omega \frac{u^\epsilon(x,T) - u^*(x,T)}{\epsilon} \, dx + \int_Q \frac{u^\epsilon - u^*}{\epsilon} \, dxdt - B \int_Q \frac{(m^* + \epsilon l)^2 - m^{*2}}{\epsilon} \, dxdt \right) \\
&= A \int_\Omega \psi(x,T) \, dx + \int_Q \psi \, dxdt - \int_Q 2Bm^* l \, dxdt.
\end{aligned}$$

Using the weak solution formulation for the adjoint problem with test function ψ, we obtain

$$\begin{aligned}
0 &\geq A \int_\Omega \psi(x,T) \, dx + \int_Q \psi \, dxdt - \int_Q 2Bm^* l \, dxdt \\
&= A \int_\Omega \psi(x,T) \, dx + \int_Q ((-p_t - (m^* - 2u^*)p)\psi + \mu \nabla p \cdot \nabla \psi) \, dxdt \\
&\qquad - \int_Q 2Bm^* l \, dxdt \\
&= \int_Q ((\psi_t - (m^* - 2u^*)\psi)p + \mu \nabla p \cdot \nabla \psi) \, dxdt - \int_Q 2Bm^* l \, dxdt \\
&= \int_Q u^* l p - 2Bm^* l \, dxdt \\
&= \int_Q l \left(u^* p - 2Bm^* \right) \, dxdt.
\end{aligned} \tag{2.5.43}$$

Taking cases on the sets where $0 < m^* < M$, $m^* = M$, and $m^* = 0$, one obtains the desired control characterization. □

2.5.4 $V_2 = \{m \in L^\infty(Q) : 0 \leq m(x,t) \leq M, \int_Q m \, dxdt = \delta\}$

To obtain a control characterization for the case with a fixed amount of resources, we once again introduce a new state variable, w in $H^1(\Omega)$ satisfying

$$\begin{aligned}
\Delta w &= \int_0^T m(x,t) \, dt \qquad \text{in} \quad \Omega \\
\frac{\partial w}{\partial \nu} &= \frac{\delta}{|\partial \Omega|} \qquad \text{on} \quad \partial\Omega.
\end{aligned} \tag{2.5.44}$$

To see how this satisfies the desired constraint, we integrate m over Q, substitute the new state and integrate by parts:

$$\begin{aligned}\int_\Omega \left(\int_0^T m(x,t)\ dt \right) dx &= \int_\Omega \Delta w(x)\ dx \\ &= \int_{\partial\Omega} \nabla w \cdot \nu\ dSdx \\ &= \int_{\partial\Omega} \frac{\partial w}{\partial \nu}\ dSdx \\ &= \delta \end{aligned}$$ □

Remark: Consider the case $n = 1$ with $\Omega = (0,1)$. Using the discrete measure, $|\partial\Omega| = 2$, and we have

$$\begin{aligned} w''(x) &= \textstyle\int_0^T m(x,t)\,dt \quad \text{in} \quad (0,1) \\ w'(0)\cdot(-1) &= \tfrac{\delta}{2} \\ w'(1)\cdot(1) &= \tfrac{\delta}{2} \end{aligned}$$

which gives the following:

$$\begin{aligned}\int_0^1 \left(\int_0^T m(x)\ dt \right) dx &= \int_0^1 w''(x)\ dx \\ &= \left(w'(x)\Big|_0^1 \right) \\ &= (w'(1) - w'(0)) \\ &= \left(\frac{\delta}{2} - \frac{-\delta}{2} \right) \\ &= \delta. \end{aligned}$$

The problem of maximizing J_2 (2.2.9) over V_2 (2.2.8) is now recast as that of maximizing J_2 (2.2.9) over U_2 (2.2.7) such that a corresponding pair u, w exists satisfying (2.2.1) together with boundary condition (2.2.2) and (2.5.44) respectively. Now we will have a system of two sensitivities, ψ_1 and ψ_2.

Theorem 2.5.7 (Sensitivity). *The mapping $m \in U_2 \mapsto (u, w)(m)$ is differentiable in the following sense: for each m, l in U_2 such that $m + \epsilon l \in U_2$ for all ϵ sufficiently small, then there exist $\psi_1 \in V, (\psi_1)_t \in V^*$ and $\psi_2 \in H^1(\Omega)$, such that*

$$\psi_1^\epsilon \rightharpoonup \psi_1 \text{ weakly in } V \text{ as } \epsilon \to 0, \tag{2.5.45}$$

$$(\psi_1^\epsilon)_t \rightharpoonup (\psi_1)_t \text{ weakly in } V^* \text{ as } \epsilon \to 0, \tag{2.5.46}$$

$$\psi_2^\epsilon \rightharpoonup \psi_2 \text{ weakly in } H^1(\Omega) \text{ as } \epsilon \to 0, \tag{2.5.47}$$

and the sensitivities ψ_1 and ψ_2 satisfy

$$\begin{aligned} \psi_{1t} - \mu\Delta\psi_1 - (m - 2u)\psi_1 &= ul \quad \text{in } Q, \\ \frac{\partial \psi_1}{\partial \nu} &= 0 \quad \text{on } \partial\Omega \times (0, T), \\ \psi_1 &= 0 \quad \text{on } \Omega \times \{t = 0\}. \end{aligned} \tag{2.5.48}$$

$$\begin{aligned} \Delta\psi_2 &= \int_0^T l\, dt \quad \text{in } \Omega, \\ \frac{\partial \psi_2}{\partial \nu} &= 0 \quad \text{on } \partial\Omega. \end{aligned} \tag{2.5.49}$$

Proof. A priori estimates on the quotients can be shown similarly to the estimates on the states. That sensitivity ψ_1 satisfies 2.5.48 is shown similar to that in Theorem (2.5.5). Let $w^\epsilon = w(m^\epsilon)$ where $m^\epsilon = m + \epsilon\ell$. The state PDEs corresponding to controls m^ϵ and m are given by

$$\Delta w^\epsilon = \int_0^T m^\epsilon\, dt \tag{2.5.50}$$

$$\Delta w = \int_0^T m\, dt \tag{2.5.51}$$

Taking differences and dividing by ϵ we have:

$$\Delta\left(\frac{w^\epsilon - w}{\epsilon}\right) = \int_0^T \ell\, dt \tag{2.5.52}$$

That is, the PDE satisfied by the difference quotient is given by

$$\Delta\psi_2^\epsilon = \int_0^T \ell \, dt \tag{2.5.53}$$

Note that ψ_2^ϵ doesn't depend on epsilon and the sensitivity ψ_2 satisfies the desired PDE. Similarly, the sensitivity functions satisfy the given boundary conditions. $\square$

Theorem 2.5.8. *Given an optimal control m^* and corresponding state (u^*, w^*), there exists (p_1, p_2) with $p_1 \in L^2(0,T,H^1(\Omega)) \cap L^\infty(Q), (p_1)_t \in L^2((0,T),H^1(\Omega)^*)$, and $p_2 \in H^1(\Omega)$ satisfying*

$$\begin{aligned} -(p_1)_t - \mu\Delta p_1 - (m^* - 2u^*)p_1 &= 1 \quad \text{in } Q, \\ \frac{\partial p_1}{\partial \nu} &= 0 \quad \text{on } \partial\Omega \times (0,T), \\ p_1 &= A \quad \text{on } \Omega \times \{t = T\}. \end{aligned} \tag{2.5.54}$$

$$\begin{aligned} \Delta p_2 &= 0 \quad \text{in } \Omega, \\ \frac{\partial p_2}{\partial \nu} &= 0 \quad \text{on } \partial\Omega. \end{aligned} \tag{2.5.55}$$

Furthermore, m^* is characterized by

$$m^*(x,t) = \min\left\{M, \max\left\{\frac{p_2(x) + (u^* p_1)(x,t)}{2B}, 0\right\}\right\} \tag{2.5.56}$$

Proof. The proof follows just as with Theorem 2.5.6 except (2.5.43) picks up an extra term for the new state:

$$\begin{aligned}
0 \geq & A\int_\Omega \psi_1(x,T)\ dx + \int_Q (1\cdot\psi_1 - 2Bm^*l)\,dxdt + \int_\Omega 0\cdot\psi_2\,dx \\
= & \int_\Omega p_1(x,T)\psi_1(x,T)\ dx \\
& + \int_Q ((-(p_1)_t - (m^*-2u^*)p_1)\psi_1 + \mu\nabla p_1\cdot\nabla\psi_1 - 2Bm^*l)\ dxdt \\
& - \int_\Omega \nabla p_2\cdot\nabla\psi_2\ dx \\
= & \int_Q (((\psi_1)_t - (m^*-2u^*)\psi_1)p_1 + \mu\nabla p_1\cdot\nabla\psi_1 - 2Bm^*l)\ dxdt \\
& + \int_\Omega p_2(x)\int_0^T l(x,t)\ dt\ dx \\
= & \int_Q u^*lp_1 - 2Bm^*l\ dxdt + \int_Q p_2(x)l(x,t)\ dxdt \\
= & \int_\Omega l(x,t)\Big((u^*p_1)(x,t) - 2Bm^*(x,t) + p_2(x)\Big)\ dxdt.
\end{aligned} \tag{2.5.57}$$

Again, by taking cases on the sets where $0 < m^* < M$, $m^* = M$, and $m^* = 0$, one obtains the desired control characterization. □

Remarks: The solution p_2 to (2.5.55) is a constant chosen in such a way that the integral constraint on m is satisfied. The results of this section are all valid for Dirichlet boundary conditions (2.2.3).

2.6 Uniqueness of Optimal Control

The coupled state and adjoint equations with initial and boundary conditions together with the control characterization form the optimality system. In this section, we show the uniqueness of solutions for each of the optimality systems in section 2.5 under condition of small T, which gives the uniqueness of the optimal control. Such a condition on T is common in optimal control with time-varying dynamics (Neilan and Lenhart, 2011; Fister, 1997, 2001; Lenhart et al., 1999).

Theorem 2.6.1. *There exists a positive number T_0 such that if $0 < T \leq T_0$, then there is a unique optimal control for the problem with control set U_2 (2.2.7) and objective functional J_2 (2.2.9).*

Proof. From the result in Section 2.4, there exists an optimal control, and corresponding adjoints and states satisfying the optimality system. Thus, it suffices to prove the uniqueness of the solutions of the optimality system as that will imply the uniqueness of the optimal control.

For $i = 1, 2$, let u_i, p_i, m_i be the states, adjoints, and controls solving the optimality system. Let $u_i = e^{\lambda t} w_i$ and $p_i = e^{-\lambda t} \pi_i$ for λ a positive constant to be chosen below. Substitution into the optimality system gives

$$\lambda w_i + (w_i)_t - \mu \Delta w_i = w_i(m_i^* - e^{\lambda t} w_i),$$

$$\lambda \pi_i - (\pi_i)_t - \mu \Delta \pi_i = \pi_i(m_i^* - 2e^{\lambda t} w_i) + 1$$

and

$$m_i^* = \min\left\{M, \max\left\{\frac{w_i \pi_i}{2B}, 0\right\}\right\}.$$

Subtracting we get

$$\lambda(w_1 - w_2) + (w_1 - w_2)_t = \mu\Delta(w_1 - w_2) + m_1^*(w_1 - w_2) + w_2(m_1^* - m_2^*)$$

$$-e^{\lambda t}(w_1 + w_2)(w_1 - w_2)$$

and

$$\lambda(\pi_1 - \pi_2) - (\pi_1 - \pi_2)_t = \mu\Delta(\pi_1 - \pi_2) + m_1^*(\pi_1 - \pi_2) + \pi_2(m_1^* - m_2^*)$$

$$-2e^{\lambda t}(\pi_1(w_1 - w_2) + w_2(\pi_1 - \pi_2)) \ .$$

Using $(w_1 - w_2)$ and $(\pi_1 - \pi_2)$ in the weak formulations respectively, we obtain

$$\int_\Omega \frac{1}{2}(w_1 - w_2)^2(x,T)\,dx + \lambda \int_Q (w_1 - w_2)^2\,dxdt + \mu \int_Q |\nabla(w_1 - w_2)|^2\,dxdt$$

$$= \int_Q (m_1^* - e^{\lambda t}(w_1 + w_2))(w_1 - w_2)^2 + w_2(m_1^* - m_2^*)(w_1 - w_2)\,dxdt$$

and

$$\int_\Omega \frac{1}{2}(\pi_1 - \pi_2)^2(x,0)\,dx + \lambda \int_Q (\pi_1 - \pi_2)^2\,dxdt + \mu \int_Q |\nabla(\pi_1 - \pi_2)|^2\,dxdt$$

$$= \int_Q (m_1^* - 2e^{\lambda t}w_2)(\pi_1 - \pi_2)^2 + \pi_2(m_1^* - m_2^*)(\pi_1 - \pi_2)$$

$$-2e^{\lambda t}\pi_1(w_1 - w_2)(\pi_1 - \pi_2)\,dxdt\ .$$

Now, we estimate $(m_1^* - m_2^*)$:

$$\begin{aligned}
|m_1^* - m_2^*| &\le \frac{1}{2B}|u_1 p_1 - u_2 p_2| \\
&= \frac{1}{2B}|w_1\pi_1 - w_2\pi_2| \\
&= \frac{1}{2B}|w_1\pi_1 - w_1\pi_2 + w_1\pi_2 - w_2\pi_2| \\
&= \frac{1}{2B}|w_1(\pi_1 - \pi_2) + \pi_2(w_1 - w_2)| \\
&= \frac{1}{2B}|\pi_1(w_1 - w_2) + w_2(\pi_1 - \pi_2)|
\end{aligned}$$

The spatial gradient terms from the left hand sides and the $e^{\lambda t}(w_1 + w_2)(w_1 - w_2)^2$ and $2e^{\lambda t}w_2(\pi_1 - \pi_2)^2$ terms from the right hand sides can be eliminated from the inequality estimates due to their signs. Using the estimate on $|m_1^* - m_2^*|$ and the upper bound on m_1^*, we have

$$\int_\Omega \frac{1}{2}(w_1 - w_2)^2(x,T)\,dx + \lambda \int_Q (w_1 - w_2)^2\,dxdt$$

$$\leq \int_Q M(w_1 - w_2)^2 + \frac{|w_2|}{2B}(|\pi_2|(w_1 - w_2)^2 + |w_1(\pi_1 - \pi_2)(w_1 - w_2)|)\, dxdt$$

$$\leq \int_Q \left(M + \frac{|w_2||\pi_2|}{2B}\right)(w_1 - w_2)^2 + \frac{|w_1||w_2|}{2B}|(\pi_1 - \pi_2)(w_1 - w_2)|\, dxdt$$

and

$$\int_\Omega \frac{1}{2}(\pi_1 - \pi_2)^2(x,0)\, dx + \lambda \int_Q (\pi_1 - \pi_2)^2\, dxdt$$

$$\leq \int_Q \Big(M(\pi_1 - \pi_2)^2 + \frac{|\pi_2|}{2B}(|w_2|(\pi_1 - \pi_2)^2 + |\pi_1(w_1 - w_2)(\pi_1 - \pi_2)|)$$

$$-2e^{\lambda t}|\pi_1||(w_1 - w_2)(\pi_1 - \pi_2)|\Big)\, dxdt$$

Summing these two inequalities and continuing to estimate we have

$$\begin{aligned}\int_\Omega \frac{1}{2}(w_1 - w_2)^2(x,T)\, dx + \lambda \int_Q \left((w_1 - w_2)^2 + (\pi_1 - \pi_2)^2\right)\, dxdt \\ + \int_\Omega \frac{1}{2}(\pi_1 - \pi_2)^2(x,0)\, dx \\ \leq \int_Q (M + \frac{|w_2||\pi_2|}{2B})\left((w_1 - w_2)^2 + (\pi_1 - \pi_2)^2\right) dxdt \\ + \int_Q (\frac{|w_1||w_2| + |\pi_1||\pi_2|}{2B} - 2e^{\lambda T}|\pi_1|)\,|(w_1 - w_2)(\pi_1 - \pi_2)|\, dxdt\end{aligned}$$

By Cauchy's inequality and the L^∞ bounds on π_i and w_i we have

$$\begin{aligned}\int_\Omega \frac{1}{2}(w_1 - w_2)^2(x,T)\, dx + \int_Q \left(\lambda - \left(C_1 + C_2 e^{\lambda T}\right)\right)\left((w_1 - w_2)^2 + (\pi_1 - \pi_2)^2\right)\, dxdt \\ + \int_\Omega \frac{1}{2}(\pi_1 - \pi_2)^2(x,0)\, dx \leq 0\end{aligned}$$

Let $\lambda > C_1 + C_2$. Then for T small enough, we get $\lambda > C_1 + C_2 e^{\lambda T}$ and, thus, $(w_1 - w_2) = (\pi_1 - \pi_2) = 0$. That is, the solution to the optimality system is unique which gives the uniqueness of the optimal control.

□

2.7 Numerical Results

Using numerical simulations, we illustrate various scenarios on a one dimensional spatial domain. Let $\Omega = (0, 1)$ and diffusion coefficient $\mu = 0.1$. Our state equation is given by

$$u_t - 0.1u_{xx} = u(m - u) \quad \text{in} \quad (0, 1) \times (0, T).$$

We will consider cases with $m = m(x, t)$ and $m = m(x)$. We emphasize Neumann boundary conditions, $u_x(0, t) = u_x(1, t) = 0$, but, in the first three scenarios, we will compare the case with Neumann boundary conditions to the case with Dirichlet boundary conditions. Our baseline initial condition represents a population concentrated in the center of the spatial domain and is shown in Figure 2.1. In two

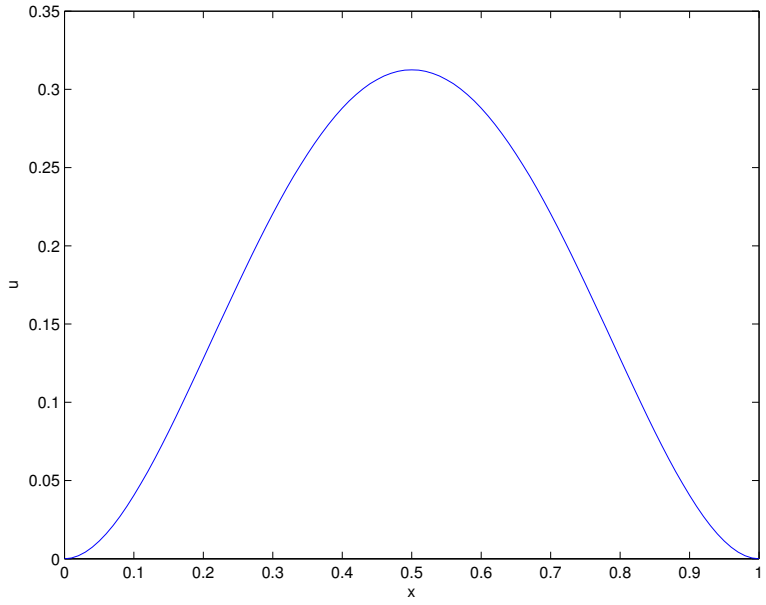

Figure 2.1: Baseline initial condition with single peak centered in the domain

scenarios we will consider different initial conditions. The baseline value for the upper bound on the control is $M = 1$. The baseline value for the final time is $T = 1$ but in two scenarios we will use $T = 0.2$. We also compare cases with and without a payoff term and with and without an integral constraint on m. Finally, for all but the last

Table 2.1: Baseline values for simulations.

Variable	Description	Baseline	Alternates
μ	diffusion coefficient	0.1	
M	upper bound on control m	1	
BCs	boundary conditions	Neumann	Dirichlet
ICs	initial conditions	Fig. 2.1	Figs. 2.3, 2.5
T	final time	1	0.2
A	weight coefficient on payoff term	0	0.5
B	weight coefficient on the cost term	0.05	0.2

scenario we consider, the value for the weight coefficient on the cost term is $B = 0.05$. These values are summarized in Table 2.1. For all scenarios, each of these baseline values hold unless stated otherwise.

Since we have an initial state condition and a final time adjoint condition, a forward-backward sweep iterative method is used to solve the optimality system (Hackbusch, 1978; Lenhart and Workman, 2007). If there is no integral constraint on the control variable m, after initializing our control, the state equation is solved forward in time and then the adjoint equation is solved backward in time. We then use the control characterization to update the control. If $m = m(x)$, the control characterization is given by equation (2.5.22),

$$m^*(x) = \min\left\{M, \max\left\{\frac{\int_0^T (u^*p)(x,t)dt}{2BT}, 0\right\}\right\}.$$

If $m = m(x,t)$, the control characterization is given by equation (2.5.42),

$$m^*(x,t) = \min\left\{M, \max\left\{\frac{(u^*p)(x,t)}{2B}, 0\right\}\right\}.$$

This process is repeated until controls from successive iterates are sufficiently close.

In the cases with an integral constraint on the control, the control characterization is given by equation (2.5.36),

$$m^*(x) = \min\left\{M, \max\left\{\frac{p_2 + \int_0^T (u^* p_1)(x,t)dt}{2BT}, 0\right\}\right\},$$

if $m = m(x)$ or by equation (2.5.56),

$$m^*(x,t) = \min\left\{M, \max\left\{\frac{p_2(x) + (u^* p_1)(x,t)}{2B}, 0\right\}\right\},$$

if $m = m(x,t)$. In these cases, we first make an initial guess for the solution to the adjoint function, p_2. Recall that this is some constant chosen so that the integral constraint, $\int_Q m\, dxdt = \delta$, is satisfied. Then the forward-backward sweep is performed as described above. We then estimate the integral of our control using a trapezoid method. The size of this integral indicates how we are to update our guess for the adjoint p_2. We repeat the entire process until the difference between the integral and δ is sufficiently small.

Finite differences are used to approximate derivatives. We use a forward difference approximation for the time derivative:

$$u_t(x,t) \approx \frac{u(x,t+\Delta t) - u(x,t)}{\Delta t}.$$

A centered difference approximation is used for the second space derivative:

$$u_{xx}(x,t) \approx \frac{u(x-\Delta x,t) - 2u(x,t) + u(x+\Delta x,t)}{(\Delta x)^2}.$$

For these simulations, we let $\Delta x = 0.01$. Choosing $\Delta t = \frac{(\Delta x)^2}{4}$, we require $\mu \leq 2$ to satisfy the CFL stability criterion for this method (LeVeque, 2007).

We begin by contrasting Neumann and Dirichlet boundary conditions for the case $m = m(x,t)$. We can see in Figure 2.2 that more control is applied for

Neumann boundary conditions than for the case with Dirichlet boundary conditions. In particular, $\int_Q m(x,t)dxdt = 0.8144$ for Neumann boundary conditions, whereas $\int_Q m(x,t)dxdt = 0.4885$ for the case with Dirichlet boundary conditions. It makes sense to invest more on allocating resources for a population not subject to an inhospitable boundary. A larger value for the objective functional is also achieved for the case with Neumann boundary conditions, 0.2056 compared to 0.1286.

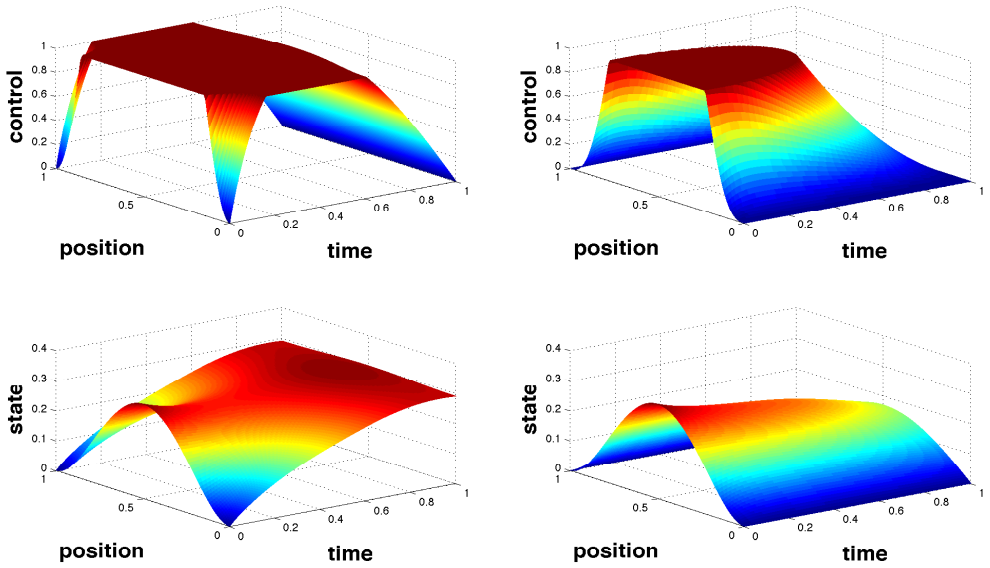

Figure 2.2: Optimal control and corresponding states for Neumann (on left) and Dirichlet (on right) boundary conditions with initial condition shown in Figure 2.1

Next we consider an initial population distribution with two peaks of the same size: one in the middle of the domain and another to one side of the domain, as shown in Figure 2.3. We again contrast the case with Neumann boundary conditions to that with Dirichlet boundary conditions. The final time has been changed to $T = 0.2$. The results are shown in Figure 2.4. In the case of Neumann boundary conditions, there is no distinction between the control levels applied to the two population concentrations. This is not the case, however, when we consider Dirichlet boundary conditions. In the figure it is clear that more control is applied to the population in the center. From an

ecological perspective, it makes sense to invest more in the population that is further away from the inhospitable boundary. The values for the objective functional at the optimal control for the two cases are 0.0396 for Neumann boundary conditions and 0.0333 for Dirichlet boundary conditions.

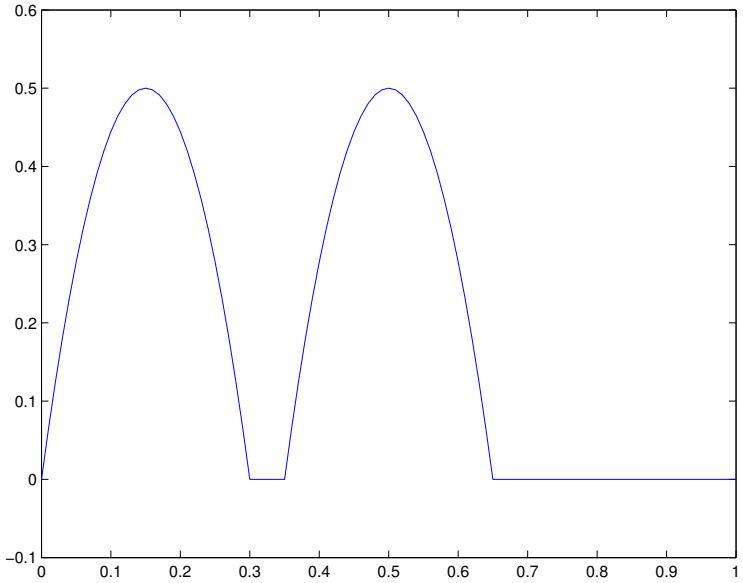

Figure 2.3: Initial condition with centered peak and peak near boundary

Next we examine how resources are optimally allocated for a population that is concentrated near an inhospitable boundary. Consider the initial condition in Figure 2.5) with Dirichlet boundary conditions and final time $T = 1$. In Figure 2.6, one can see how an optimal control will "drive" the population toward the center of the domain and away from the hostile boundary.

For the remaining cases we only consider Neumann boundary conditions and the baseline initial condition shown in Figure 2.1. Figure 2.7 compares the cases with $m = m(x, t)$ and varying values for the final time, $T = 1$ and $T = 0.2$ respectively. We see that in the case with more time, more control is applied early in the time domain compared to the same interval of time for the other case. Ecologically, it is worthwhile to invest more in resources if there is more time to allocate them. The

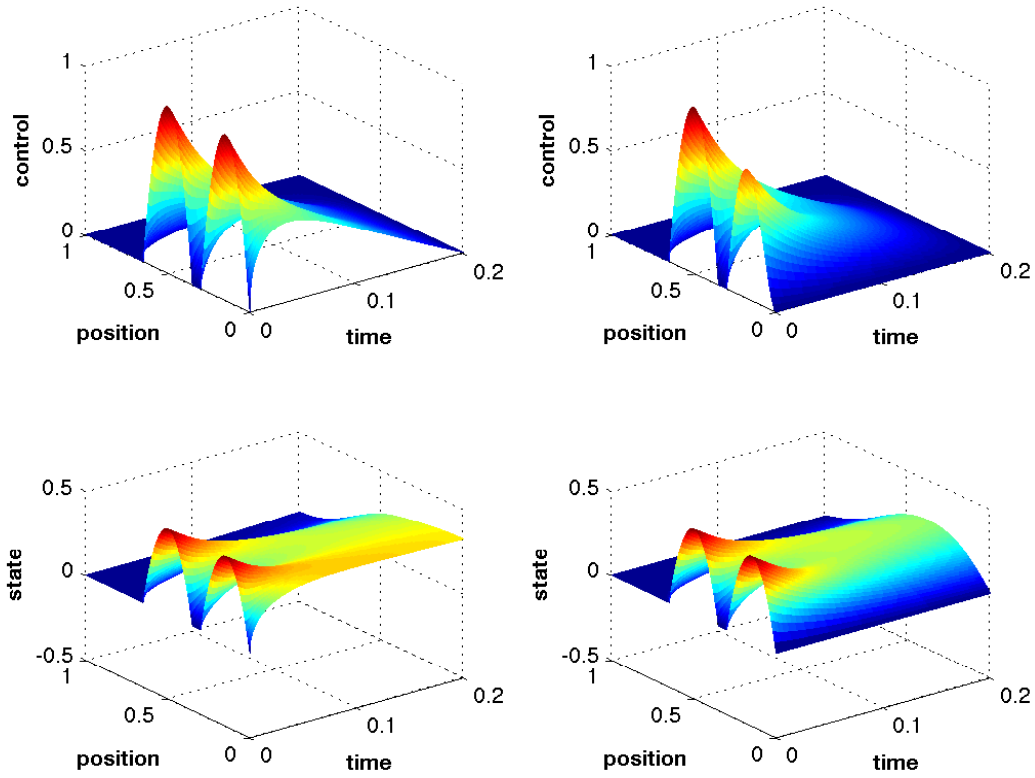

Figure 2.4: Optimal control and corresponding states for Neumann (on left) and Dirichlet (on right) boundary conditions with initial condition shown in Figure 2.3, $T = 0.2$

values for the objective functional at the optimal control for the two cases are 0.2056 for $T = 1$ and 0.0331 for $T = 0.2$.

The remaining cases all have final time $T = 1$. Comparing the case where the control is a function of both time and space to the case where the control is constant in time illustrates that, with the ability to vary the control in time, one can achieve a larger value for the objective functional. In Figure 2.8, the value of the objective functional for the space and time varying case is $J = 0.2056$ while the value of the objective functional for the constant in time case is $J = 0.2000$.

We now compare cases with and without an integral constraint on the control. An integral constraint will have an impact on the form of the optimal control. In

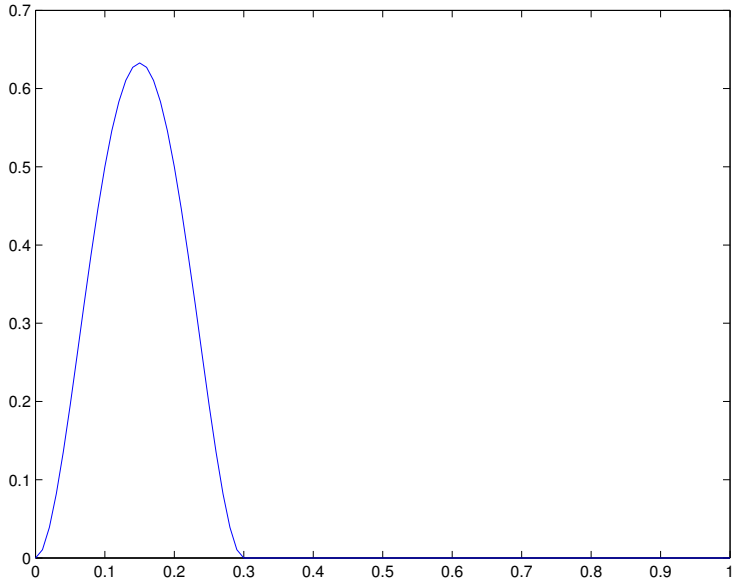

Figure 2.5: Initial condition with single peak near boundary

Figure 2.9 we compare these two cases for $m = m(x,t)$. In this case the constraint is given by

$$\int_Q m(x,t)\ dxdt = 0.3.$$

We see that under the integral constraint, the control is applied early; the control equals zero beyond $t = 0.6$. With a fixed amount to invest, it is optimal to invest it all early. Furthermore, less control is applied where the population concentrations are small than in the case with no integral constraint. For comparison, we note that the total integral of m over Q for the case without the integral constraint is $\int_Q m(x,t)\ dxdt = 0.8$. The values for the objective functional for the cases with and without the integral constraint are $J = 0.2056$ and $J = 0.1861$ respectively. If, in addition to an integral constraint, we restrict the control such that $m = m(x)$, the value of the objective functional is $J = 0.1739$ (see left side of Figure 2.10). One can see how the value of the objective functional at the optimal control decreases when there is an integral constraint and decreases further when the control can only vary

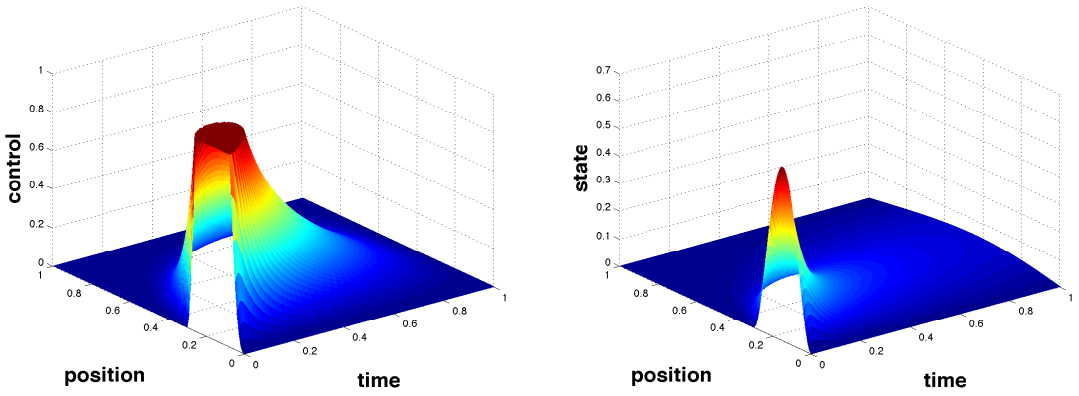

Figure 2.6: Optimal control and corresponding state for Dirichlet boundary conditions with initial condition shown in Figure 2.5, $T = 1$

in space, which is expected since these two optimal controls are admissible controls in U_2. Figure 2.10 shows the two cases $m = m(x,t)$ and $m = m(x)$ with each having an integral constraint on m. As noted above, it is optimal to invest the allotted control amount early. When the control is restricted to varying in space only, this is no longer possible. While the amount of resource allocated for both of these cases is the same, the overall population abundance, $\int_Q u(x,t)\,dxdt$, is 0.1975 for $m = m(x,t)$ compared to 0.1810 for $m = m(x)$.

Figure 2.11 illustrates the cases with and without an integral constraint on the control but with $m = m(x)$ in both cases. In this case the constraint is given by

$$\int_Q m(x)\,dxdt = 0.3.$$

The values for the objective functional for the cases with and without the integral constraint are $J = 0.2000$ and $J = 0.1739$ respectively. The total integral of m over Q for the case without the integral constraint is $\int_Q m(x)\,dxdt = 0.9737$.

Finally, we consider cases involving a final time payoff term in the objective functional. The weight coefficient on this term in the objective functional is $A = 0.5$. For the case where $m = m(x,t)$, the final time population size, $\int_\Omega u(x,T)\,dx$, is

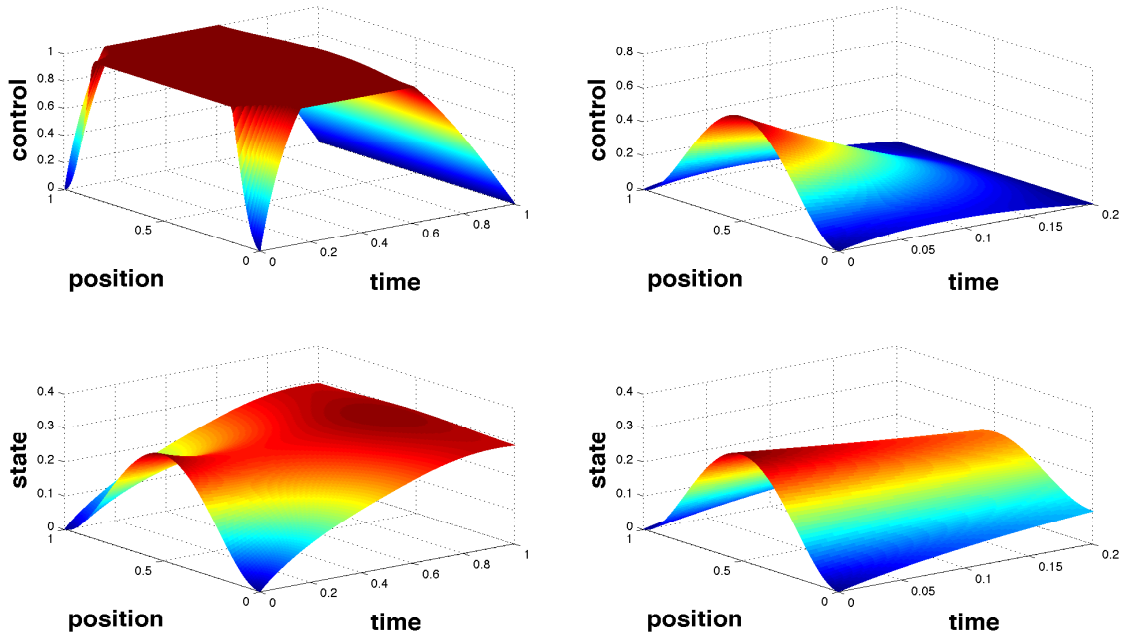

Figure 2.7: Optimal control and corresponding states for Neumann boundary conditions with initial condition shown in Figure 2.1 and varying final time $T = 1$ (on left) and $T = 0.2$ (on right)

0.2946 when there is no final time payoff term compared to 0.3494 when there is a final time payoff term. This is illustrated in Figure 2.12. One can see the effect of the payoff term on the states. The state surface at the final time for the case with the payoff term (on the right) is higher than the state surface at the final time for the case without the payoff term (on the left). The effect on the corresponding controls is also evident. The presence of the payoff term in the objective functional in this case results in the application of maximum control for nearly the entire space-time domain. The values for the objective functional at the optimal control for these two cases are 0.2056 for $A = 0$ and 0.3747 for $A = 0.5$.

These observations hold also for the case where $m = m(x)$. The final time population size, $\int_\Omega u(x,T)\,dx$ is 0.3431 when there is no payoff term, compared to 0.3495 when there is a payoff term. This is illustrated in Figure 2.13. The state

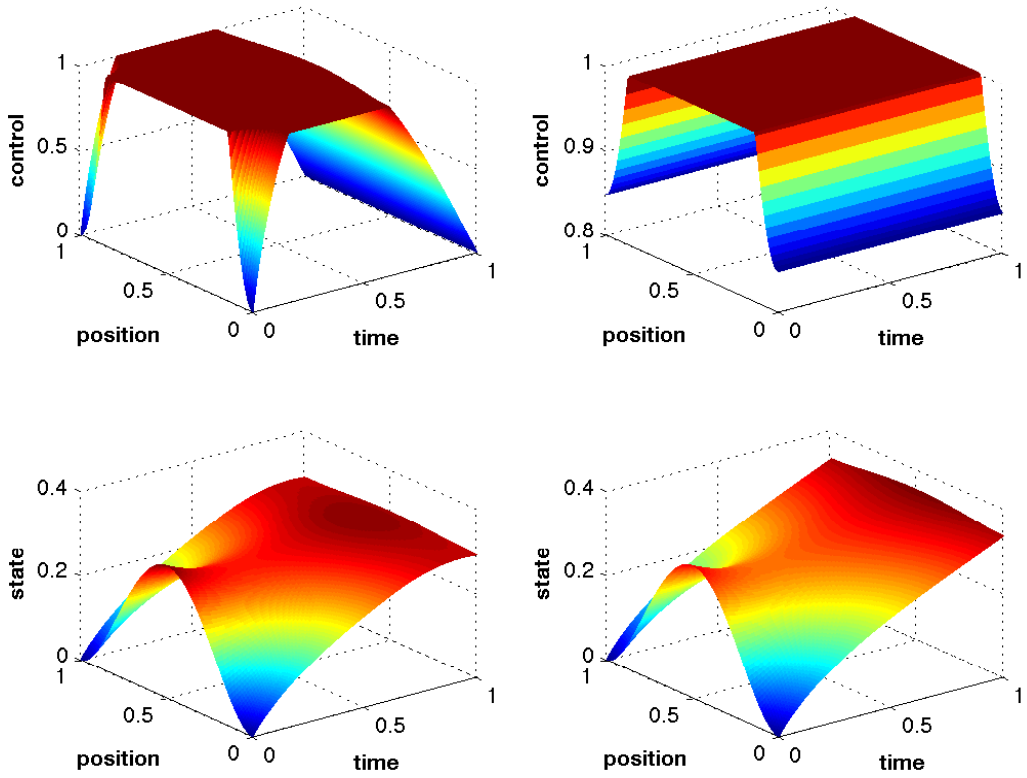

Figure 2.8: Optimal control and corresponding states for Neumann boundary conditions with initial condition shown in Figure 2.1 and with controls $m = m(x,t)$ (on left) and $m = m(x)$ (on right)

surface at the final time for the case with the payoff term (on the right) is higher than the state surface at the final time for the case without the payoff term (on the left). The presence of the payoff term in the objective functional in this case results in the application of maximum control over the entire space-time domain. The values for the objective functional at the optimal control for these two cases are 0.2000 for $A = 0$ and 0.3746 for $A = 0.5$.

Recall that the weight coefficient on the quadratic cost has been $B = 0.05$ for all of the cases illustrated thus far. If we choose a higher weight coefficient on the quadratic cost, the result is different. Figure 2.14 illustrates the case for $B = 0.2$. The case without a final payoff term is on the left and the case with a payoff term is

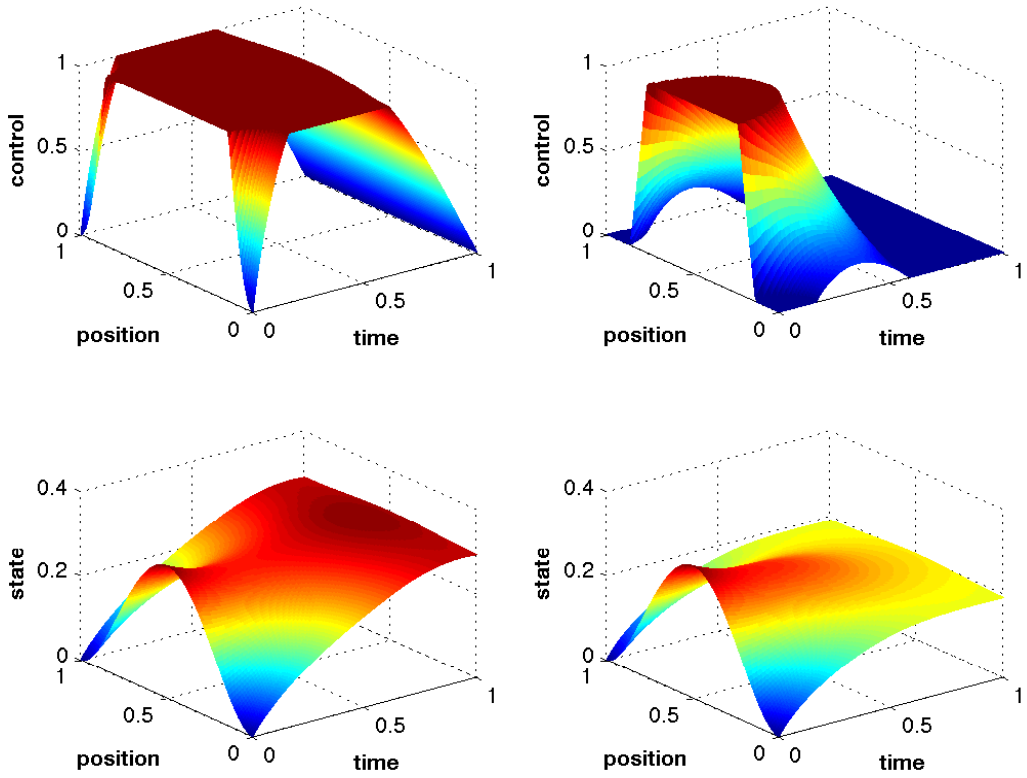

Figure 2.9: Optimal control and corresponding states for Neumann boundary conditions with initial condition shown in Figure 2.1 and controls $m = m(x,t)$ without (on left) and with (on right) an integral constraint

on the right. With a higher cost on the control, the maximum control rate, $M = 1$, is never applied. As before, the presence of the final payoff term does impact the state. The final time population size, $\int_\Omega u(x,T)\,dx$ is 0.1719 when there is no final payoff term compared to 0.2272 when there is a final payoff term. The values for the objective functional at the optimal control for the two cases are 0.1606 for $A = 0$ and 0.2584 for $A = 0.5$.

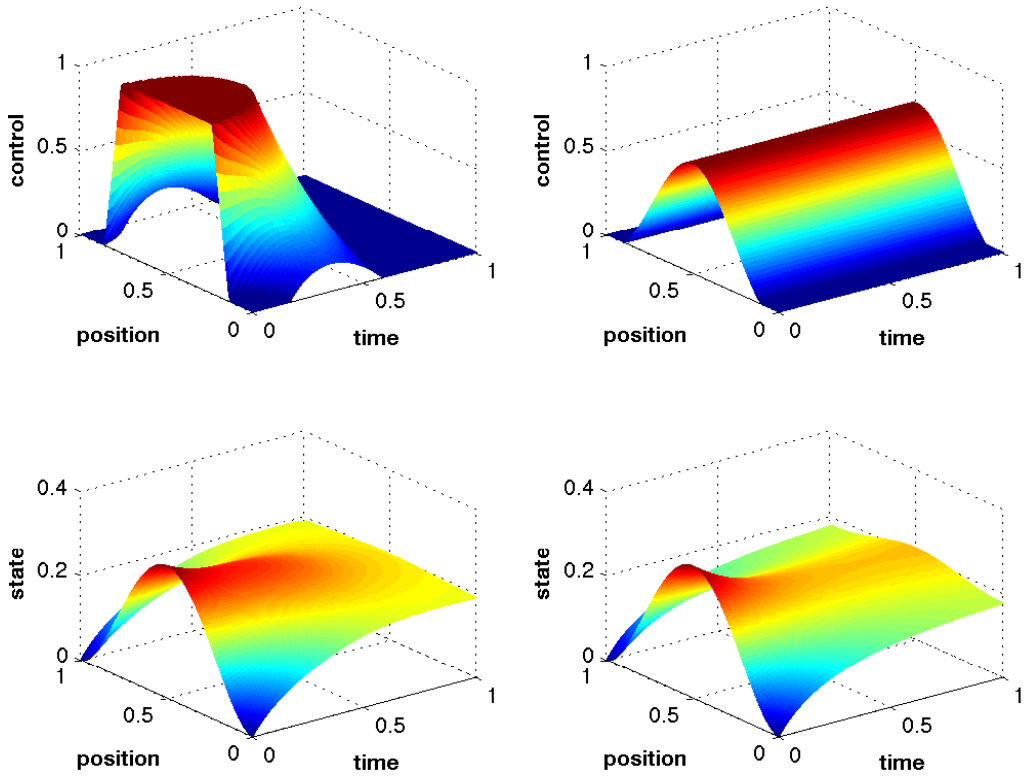

Figure 2.10: Optimal control and corresponding states for Neumann boundary conditions with initial condition shown in Figure 2.1 and controls $m = m(x,t)$ (on left) and $m = m(x)$ (on right), both with an integral constraint

2.8 Conclusions

We have considered the problem of optimal resource allocation for a diffusive population with logistic growth. Optimal resource allocation will maximize the total population over time and space including a final time population abundance goal, while minimizing the associated costs for control. We have established the existence and uniqueness of the solution to the state system given a control and we have established the existence of an optimal control. We derived necessary conditions for an optimal pair giving rise to an optimality system consisting of the coupled state-adjoint

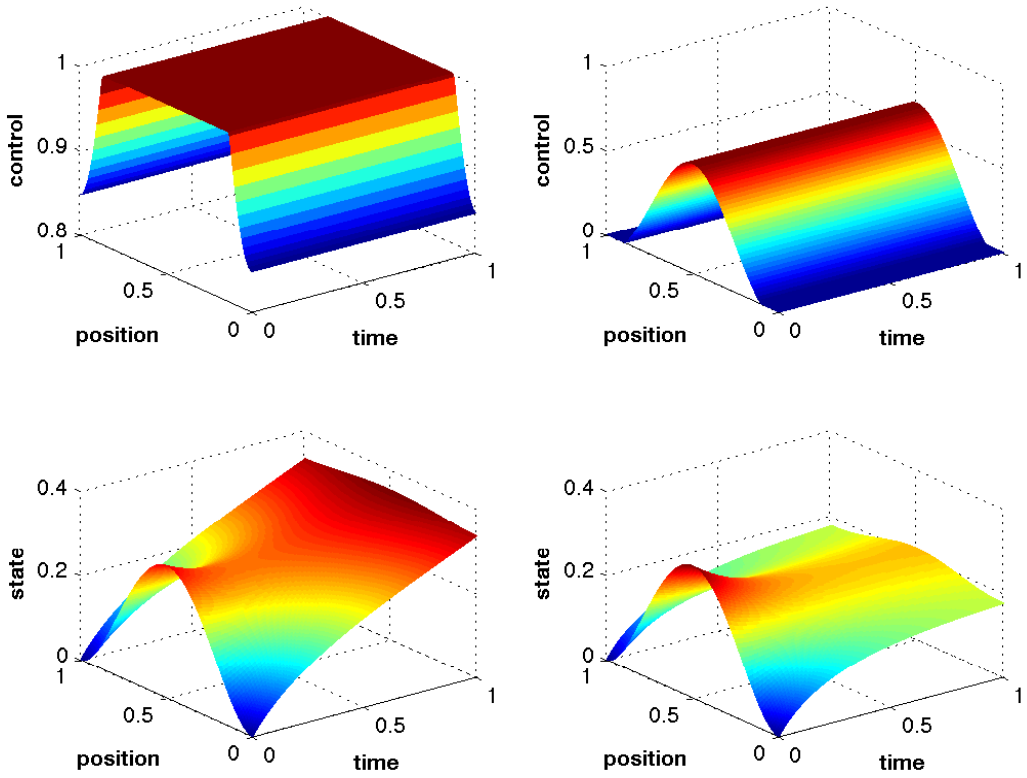

Figure 2.11: Optimal control and corresponding states for Neumann boundary conditions with initial condition shown in Figure 2.1 and controls $m = m(x)$ without (on left) and with (on right) an integral constraint

system and the characterization of the optimal control. Further, for sufficiently small values of final time T we have demonstrated uniqueness of the optimal control.

Some numerical simulations have been given to demonstrate possible scenarios. We show results for a one dimensional domain that compare Neumann and Dirichlet boundary conditions with various initial conditions as well as various final times and maximum control values for the case where $m = m(x,t)$. In particular, we showed that it makes sense to invest more on allocating resources for a population not subject to an inhospitable boundary. In the case of an inhospitable boundary, it makes sense to invest more for population densities that are further away from the inhospitable boundary than for population densities that are near the inhospitable

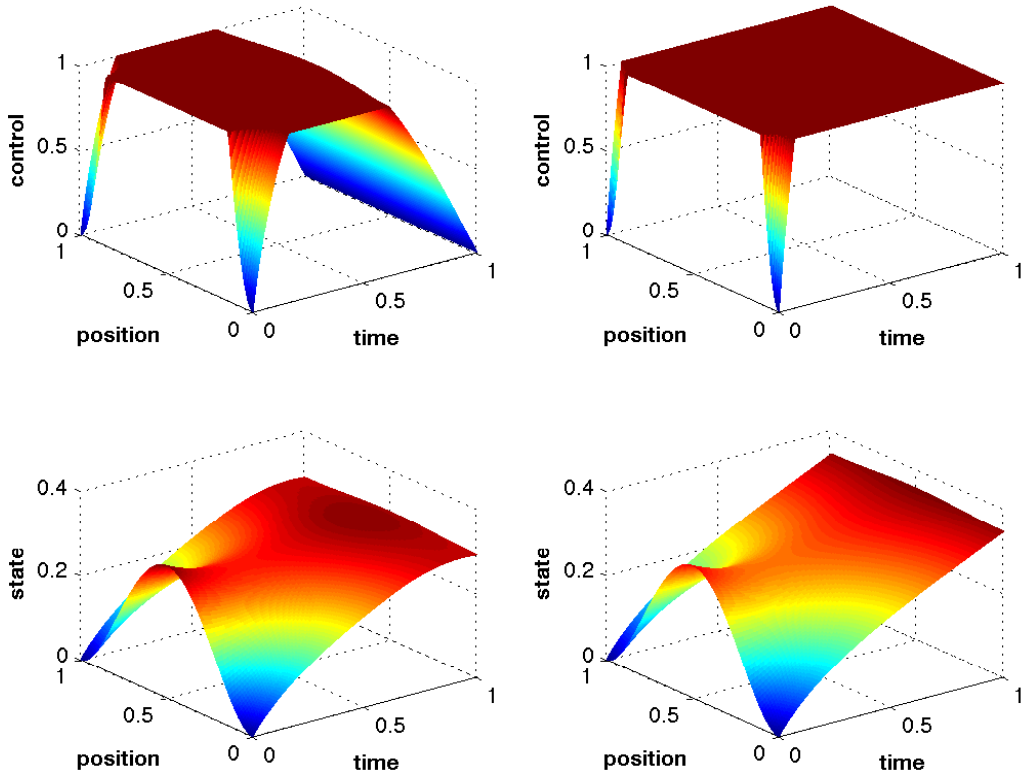

Figure 2.12: Optimal control and corresponding states for Neumann boundary conditions with initial condition shown in Figure 2.1 and controls $m = m(x,t)$ without (on left) and with (on right) a final time payoff with weight coefficient $A = 0.5$

boundary. Furthermore, an optimal control will "drive" population densities that are near an inhospitable boundary toward the center of the domain, away from the hostile boundary.

For Neumann boundary conditions, we have shown a range of comparisons for controls that vary in space and time or controls that vary only in space, for controls with and without an integral constraint, and for objective functionals with and without a final time payoff term. We showed how varying the final time can impact the optimal control. With more time, more control is applied early in the time domain compared to the same interval of time for the case with less time. Ecologically, it is worthwhile to invest more in resources if there is more time to allocate them.

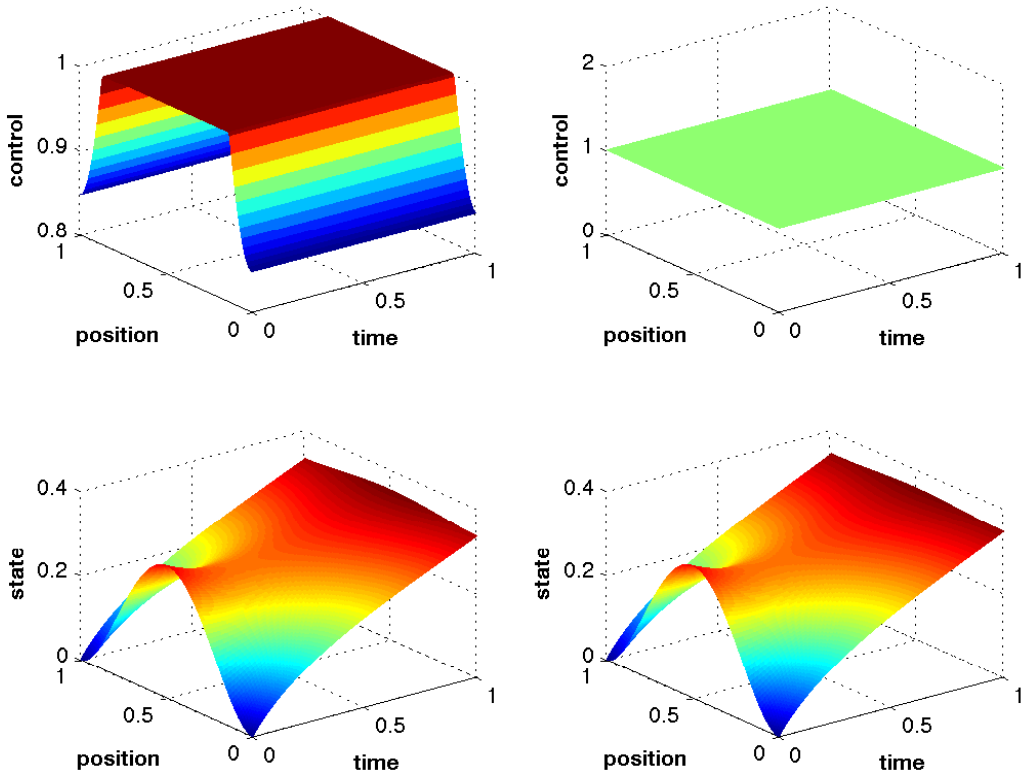

Figure 2.13: Optimal control and corresponding states for Neumann boundary conditions with initial condition shown in Figure 2.1 and controls $m = m(x)$ without (on left) and with (on right) a final time payoff with weight coefficient $A = 0.5$ and cost coefficient $B = 0.05$

We also showed how an optimal control that can vary in both time and space achieves a higher objective functional value than an optimal control that can vary in space only. The value of the objective functional decreases further under an integral constraint on the control. Furthermore, we showed that under an integral constraint, control is applied early (if $m = m(x,t)$) and less control is applied where the population concentrations are small than in the case with no integral constraint. Under the same integral constraint, we showed that a control that can only vary in space achieves a smaller overall population abundance. Finally, we showed the impact of a final time payoff term on both the optimal control and its corresponding state.

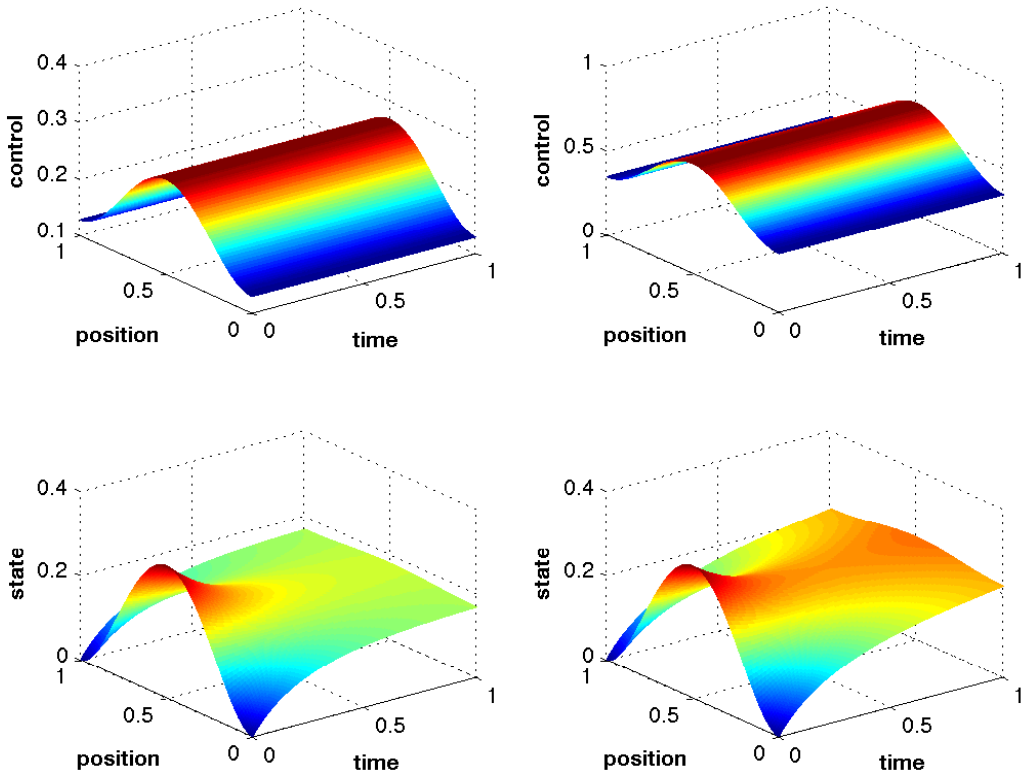

Figure 2.14: Optimal control and corresponding states for Neumann boundary conditions with initial condition shown in Figure 2.1 and controls $m = m(x)$ without (on left) and with (on right) a final time payoff with weight coefficient $A = 0.5$ and cost coefficient $B = 0.2$

There are several questions we are currently investigating that extend these results. In particular, we are considering populations with dynamics that are subject to diffusion varying in space and time as well as advection. We are also considering two dimensional habitats and ecologically more realistic initial conditions for numerical simulations as well as scenario-specific parameter values in our model and for our objective functional.

Chapter 3

Antimicrobial Stewardship for the Control of *Clostridium difficile* Transmission in Healthcare Settings

3.1 Introduction

Healthcare-associated infections (HAI) are a very significant problem in the U.S. health care system, exacting a severe cost in both lives and dollars (U.S. Department of Health and Human Services, 2013). The most common cause of HAI in the U.S. is the enteric pathogen, *Clostridium difficile* (Lessa et al., 2015). *Clostridium difficile* is an important nosocomial enteric, spore-forming bacillus (Leffler and Lamont, 2015). *Clostridium difficile* infection (CDI) can be acquired in healthcare settings as well in the community (Steiner et al., 2012). In particular, C difficile accounts for up to 20% of nosocomial antibiotic associated diarrhea and is the primary cause antibiotic-associated colitis (Bartlett, 2002). In 2011, the number of infections was estimated to be about 500,000 and the number of deaths linked to the pathogen was estimated

at 29,000 (Lessa et al., 2015). The incidence of CDI in the U.S. healthcare system continues to rise. The rate of discharges in which the patient received the diagnosis of CDI more than doubled from 2001 to 2010 (Steiner et al., 2012). The cost attributable to CDI in U.S. acute care facilities is estimated to be as much as $4.8 billion per year (Dubberke and Olsen, 2012).

CDI prevention measures have not changed sufficiently to manage these rising numbers. The focus of these measures is on testing symptomatic patients in order to identify patients with CDI so that isolation and contact precautions can be taken (Cohen et al., 2010; Dubberke et al., 2008). Recent studies, however, point out the significance to transmission within the ward of both transmission pathways beyond the ward itself and additional sources of CDI infections (Dubberke et al., 2014). Successful control measures will come only with a better understanding of *C. difficile* transmission.

Mathematical models have been developed to describe nosocomial transmission; these studies, in particular, used ordinary differential equations (ODEs) to model the transmission dynamics (Brauer, 2015; Webb et al., 2004; Yahdi et al., 2012; Hsieh et al., 2014). In a study closely related to our work, Lanzas et al. (2011) developed and analyzed an ODE model for *C. difficile* transmission within a medical ward. A threshold value for within ward transmission assuming no admission of colonized or diseased individuals was calculated. One may think of this as the relative contribution of the hospital ward *itself* to transmission with respect to some larger population. For about half of the parameter space domain, this threshold value is less than one. That is to say that in the absence of the admission of colonized and diseased patients, the basic reproductive number, R_0, is less than one. The basic reproductive number in this case is defined as the average number of secondary infections caused by the introduction of a single infected individual into a disease free hospital. Nosocomial colonizations of *C. difficile* cannot, therefore, be sustained solely by transmission due to diseased patients. The role of asymptomatic carriers, for example, is significant to within-ward transmission. Lanzas and Dubberke (2014) developed an agent-based

model (ABM) to study the effectiveness of identifying asymptomatic carriers by screening upon admission in reducing the incidence of CDI. Sources of transmission heterogeneity such as the admission of colonized and undetected diseased patients are significant in sustaining nosocomial transmission. A better understanding of transmission, therefore, requires a better understanding of the patients' pre-admission history with respect to factors pertinent to CDI and how these factors contribute to within-ward transmission.

Another important source of nosocomial transmission heterogeneity is environmental heterogeneity (Dubberke et al., 2008; Gerding et al., 2008). The risk of a susceptible patient becoming colonized by *C. difficile* depends significantly on the local pathogen contamination level (Dubberke et al., 2014). Healthcare workers are an important vector of transmission and, so, the scope of their interactions with patients represents a local pathogen contamination level (McMaster-Baxter and Musher, 2007; Donskey, 2010). The level of contamination in one hospital ward, for example, may vary significantly from that of another ward in the same hospital. One important control measure that addresses local contamination levels is to place symptomatic patients under quarantine in order for contact precautions to be initiated that decrease the environmental bioburden associated with diarrhea (Gerding et al., 2008). Cleaning and disinfection of the environment are also important control measure for reducing local contamination levels (Gerding et al., 2008).

Antibiotic treatments in hospitals provide another source of transmission heterogeneity. The fact that *Clostridium difficile* is resistant to a wide range of antibiotics allows it to colonize a gut wherein the flora has been altered due to treatment by such antibiotics (Rupnik et al., 2009). The risk factors associated with different antibiotics with respect to CDI vary significantly (Slimings and Riley, 2014; Dancer et al., 2013). Antibiotic stewardship programs are, therefore, important for the prevention and control of CDI (Feazel et al., 2014; Talpaert et al., 2011).

In this modeling study we will take into account these sources of heterogeneity in order to better understand transmission and, thereby, more accurately evaluate the

efficacy of control measures. In particular, our model includes individual patient characteristics important to pathogen transmission. We also incorporate certain stochastic effects that are significant to transmission dynamics in small populations such as a hospital. Agent-based models are well suited to simulate such individual (or agent) characteristics and behaviors as well as incorporating various stochastic effects. A recent example relevant to this study is found in D'Agata et al. (2007). Their ABM considered three processes: admission and discharge of patients, infection of patients by health-care workers (HCW) and contamination of HCW by patients. It considered only one individual trait, the bacterial load of infected patients. The goal of their study was to describe the complexities of the transmission dynamics in order to "identify the key parameters contributing to the spread of a typical antimicrobial resistant bacteria in a typical hospital setting." Notably absent from this work, however, were important individual patient characteristics such as patient history that are more important with respect to CDI than for other healthcare-associated infections. Critically important to within-ward transmission is the precise state of individual patients with respect to CDI upon admission. Patients who are colonized upon admission, for example, are a significant source contributing to within-ward transmission (Curry et al., 2013).

D'Agata et al. (2007) also lacks within-hospital patient history such as when antibiotic treatment began and what level of risk is associated with this antibiotic. This is also the case for the ABM found in Codella et al. (2015). The probability associated with a susceptible patient becoming colonized varies significantly with the both of these factors and should not be considered constant (Slimings and Riley, 2014; Dancer et al., 2013; Feazel et al., 2014; Talpaert et al., 2011). Not only are such components important for understanding transmission, they are important for intervention and control measures.

The ABM model found in Rubin et al. (2013) features several components that are important for transmission such as patient-HCW interactions, room contamination and hand hygiene. This study also incorporates antibiotic treatment. It does not,

however, consider antimicrobial stewardship as a control measure. In an evidence-based systematic review, Hsu et al. (2010) conclude that antimicrobial stewardship is one of the control measures with the greatest evidence for preventing healthcare-associated CDI and, so, in this study we consider antimicrobial stewardship as a control measure.

The goal of this study is to evaluate the efficacy of various control measures aimed at reducing environmental contamination and mitigating the effects of antibiotic use on transmission for reducing the nosocomial incidence of colonization and infection. We, therefore, propose and implement an ABM for *Clostridium difficile* transmission in hospitals that accounts for several additional processes and individual factors that are relevant to *Clostridium difficile* transmission in healthcare settings, including the environmental and antibiotic heterogeneities discussed above. Environmental decontamination strategies (Gerding et al., 2008) will result in lower probabilities of susceptible patients becoming colonized which, in turn, will further contribute to the decontamination of the environment. We account for local contamination levels in our ABM which contribute to the probability of colonization. These levels are influenced in our model by the probability of effective cleaning and this, then, is a control for modeling environmental decontamination.

There are two basic strategies employed in the implementation of an antimicrobial stewardship program (Dancer et al., 2013; Feazel et al., 2014; Talpaert et al., 2011; Gerding et al., 2008). One strategy is to reduce the overall number of antibiotic prescriptions by some proportion. This will result in a smaller number of susceptible patients and will lead, therefore, to a smaller number of colonizations. Alternatively, the relative proportions of antibiotics prescribed by *type* are changed. In particular, we are interested in differentiating antibiotics by the level of CDI risk with which they are associated. This will result in lower probabilities of susceptible patients becoming colonized. We account for both the number and type of antibiotic treatments given to patients in our model and thereby they are controls for modeling antimicrobial stewardship. In order to describe the model in such a way that facilitates replication,

we use the updated ODD (Overview, Design concepts, Details) protocol described in Grimm et al. (2010).

3.2 ODD Protocol: Overview

3.2.1 Purpose

We present an agent-based model (ABM) that simulates the transmission of *Clostridium difficile* in healthcare settings in order to evaluate the efficacy of various control measures (e.g. antimicrobial and environmental stewardship) in reducing the nosocomial incidence of colonization and infection.

3.2.2 Input Data

The model layout and agent behaviors as well as rate parameters and initial conditions come from published studies as well as previously collected epidemiological data from Barnes-Jewish Hospital in St. Louis, Missouri. These data are for a retrospective cohort of 11046 admissions in medicine wards at a large tertiary care hospital, which included laboratory-confirmed cases of CDI, admission, discharge, and confirmed laboratory dates, and antimicrobial exposures. Summary data from this set were provided by Lanzas and further description of these can be found in Lanzas et al. (2011).

Control measures for reducing nosocomial colonization and infection are model inputs. The level of contamination is one factor contributing to the probability of a susceptible patient becoming colonized. We regard effective cleaning to be cleaning that reduces the contamination level of a ward room (see Section 3.3.6). The probability that a vacant room will be effectively cleaned (terminal cleaning) is a global variable. Changing the value of this probability is a control input for the model representing different cleaning programs.

Another control strategy of the model is to reduce the overall number of antibiotic treatments by a certain proportion. This is implemented in the following way. Let q be the proportion reduction to be implemented. Of all the patients that were assigned to receive a treatment each half day according to the half-daily probability of receiving an antibiotic (see Table 3.2), only $1-q$ of them will now actually receive a treatment.

Alternatively, one may change the relative proportions of the types of antibiotic treatments that are prescribed. Each time an antibiotic treatment is prescribed, there is a probability that it will be low, high, or very-high risk with respect to CDI. The baseline values for these probabilities were taken from the data and are $0.4, 0.26$ and 0.34 respectively (see Table 3.2). These proportions can be changed in accordance with a specified stewardship program.

3.2.3 Entities, State Variables, and Scales

The model has two kinds of entities: hospital patients and rooms. Individual rooms are classified by two state variables. A room has a certain level of contamination – low, medium, or high – and a room either is or is not occupied by a patient under quarantine. Symptomatic patients are placed in quarantine or isolation for the purpose of implementing contact precautions that decrease the environmental bioburden associated with diarrhea (Gerding et al., 2008). While healthcare workers are not agents of this model, their effect as vectors for disease transmission is implicit in the fact that ward-level contamination levels contribute to patient colonization. That is, the probability that a susceptible patient in a particular ward room will become colonized depends in part on the contamination level of the entire ward. We regard a hospital ward a reasonable measure of the scope of a healthcare worker's interaction with patients.

Patients are classified by several state variables. These are summarized in Table 3.1. With respect to *Clostridium difficile* infection (CDI), a patient can be resistant to colonization, susceptible to colonization, colonized, or diseased. Each

patient is assigned a (hospital) length of stay (LOS) and the patient's time since being admitted is tracked. The time since a patient's current disease status is tracked. If a patient goes on an antibiotic, the time since beginning the antibiotic treatment is tracked as well as the level of CDI risk associated with the antibiotic with which they are being treated. This model considers three such levels of risk – low, high, and very high risk. The number of antibiotics a patient has received during hospitalization is also tracked. Colonized patients either will or will not mount an immune response. Those who will not are said to be immunocompromised. Diseased patients either will or will not be identified as diseased upon screening and those that are treated for the disease either will or will not be treated successfully.

We here describe the model's global variables. A summary of these global variables and their values is given in Table 3.2. The occupancy level for the hospital is a global variable set to 0.85. The probability of a patient being resistant upon admission is 0.58 while the probability of being diseased upon admission is 0.01. The probability of being susceptible upon admission is chosen randomly from a uniform distribution ranging from 0.21 to 0.40. This value will fix the corresponding probability of being colonized upon admission which will range between 0.01 and 0.20. The probability that a colonized patient will be immunocompromised is a global variable. The baseline value for this variable is 0.10. There is a half-daily probability that a susceptible patient or a colonized patient that is not immunocompromised will regain resistance. The *minimum* such probability is a global variable, and its value is 0.2. For a full description see Section 3.3.4. There is a half-daily probability that a patient will begin an antibiotic treatment. The baseline value for this variable is 0.27. This value was chosen so that simulation outputs pertaining to overall number of antibiotic treatments per patient reflect the hospital dataset. Each time an antibiotic treatment is prescribed, there is a probability that it will be low, high, or very-high risk with respect to CDI. The baseline values for these probabilities were taken from the data and are $0.4, 0.26$ and 0.34 respectively. The odds ratio values for high and very-high risk antibiotics are global variables and are given by $OR_h = 4$ and $OR_{vh} = 8$,

Table 3.1: Description of room and patient variables of the agent based model.

Variable	Description	Values
number-ward-rooms	number of rooms per ward	35
contamination-status	room-level contamination measure	$0, 1, 2$
contamination-quotient	ward-level contamination measure	$0, 1, ..., 70$
quarantine-patient-here	indicates whether the occupant is under quarantine	Yes, No
length-of-stay	patient's hospital length of stay	$[0, 160]$
time-since-admission	patient's time since being admitted	$0, 1, 2, ...$
disease-status	patient disease status	R,S,C,D
time-since-current-status	patient's time since their current disease status	$0, 1, 2, ...$
time-since-began-antib	patient's time since beginning their current antibiotic treatment	$0, 1, 2, ...$
treatment-length	prescribed length of the current antibiotic treatment	14
time-to-normal	time until patient's gut flora is considered normal	
	low risk:	28
	high risk:	28
	very-high risk:	70
antib-risk-level	risk level of the current antibiotic with respect to CDI	low, high, very-high
number-hosp-antibs	number of hospital antibiotics the patient has received	$0, 1, 2, ...$
immunocompromised	indicates if a colonized patient is immunocompromised	yes, no
prob-regaining-resistance	probability of regaining resistance to colonization	$[0, 1]$
prob-becoming-colonized	probability of becoming colonized	$[0, 1]$
length-incubation-period	length of time between colonization and becoming diseased by antibiotic risk level	
	low risk:	$[20, 60]$
	high risk:	$[14, 40]$
	very-high risk:	$[8, 20]$
time-until-diseased	time until an immunocompromised, colonized patient will become diseased	$[0, 60]$
will-ID	determines whether a particular screening will correctly test positive for CDI	yes, no
will-treat-succ	determines whether a patient will be successfully treated for CDI	yes, no

respectively. For a full description see Section 3.3.8. The half-daily probability of a susceptible patient becoming colonized given that they are being treated with a low risk antibiotic in a highly contaminated environment, denoted by p_ℓ^h, is a global variable and its value is 0.15. Again, for a full description see Section 3.3.8. Each time a room is cleaned, there is a probability that it will be cleaned effectively. For a description of what this means see Section 3.3.6. A baseline value of 0.5 was assigned to this variable under the simple assumption that different cleaning measures could be more or less effective at reducing the level of contamination. In our model it is assumed that patients with CDI are also symptomatic. Once a patient becomes diseased and, thus, symptomatic, they are screened for CDI. The sensitivity (0.91) of this test is a global variable as well as the turnover time (2 half-days) for this test (Planche et al., 2008). When a patient is treated for CDI, there is a probability (0.8) that the treatment will be successful.

The spatial scale of the model is one hospital consisting of six medical wards, each containing thirty-five rooms. This is reflective of the hospital from which the previously described dataset came. In this model we assume that at most one patient can occupy a room. The time step is one half-day and the temporal extent of the simulation is one year.

3.2.4 Process Overview and Scheduling

The following process takes place each time step (half-day). Time-tracking characteristics for patients are updated. New patients are admitted, the contamination of the environment is updated, the patients progress with respect to their infection status, patients are discharged, and vacant rooms are cleaned.

3.2.5 Initialization

The model hospital is initially populated with patients who have various hospital and pre-hospital histories with respect to each of the patient variables listed in Table 3.1.

Table 3.2: Description of global variables of the agent based model.

Variable	Description	Baseline Value
occupancy	occupancy level of the hospital	0.85
prob-R	probability a patient is resistant upon admission	0.58
prob-S	probability a patient is susceptible upon admission	$[0.21, 0.40]$
prob-C	probability a patient is colonized upon admission	$[0.01, 0.20]$
prob-D	probability a patient is diseased upon admission	0.01
immcomp-prob	probability a colonized patient is immunocompromised	0.1
p_{min}	minimum probability of regaining resistance	0.2
prob-antib	half-daily probability that a patient will begin an antibiotic treatment	0.27
prob-low-risk	probability a hospital assigned antibiotic is low-risk with respect to CDI	0.4
prob-high-risk	probability a hospital assigned antibiotic is high-risk with respect to CDI	0.26
prob-vhigh-risk	probability a hospital assigned antibiotic is very high-risk with respect to CDI	0.34
OR_h	odds ratio value for high risk antibiotics	4
OR_{vh}	odds ratio value for very-high risk antibiotics	8
p_ℓ^h	probability of becoming colonized if treated with low risk antibiotic in highly contaminated environment	0.15
prob-eff-clean	probability of effective cleaning	0.5
sensitivity	sensitivity of the screening test for CDI	0.91
turnover	turnover time for the screening test for CDI	2
prob-succ-treat	probability of successful treatment of CDI	0.8

The occupancy level is a global variable set to 0.85 and is kept constant. The environment is then initialized (see Section 3.3.3 for details). As the patients from this initial population are discharged, new patients are admitted. The hospital-history of these new patients more accurately reflect the processes of the model. In order for the initial hospital population not to have influence on model outputs, the simulation runs 200 time steps before recording outputs.

3.3 ODD Protocol: Submodels

This section describes in detail the subroutines that make up the main process.

3.3.1 Update Time Characteristics

Patients' time since admission and, with one exception, time since current disease status are updated. For resistant patients, the time since current disease status is not tracked. This is because the value of this state variable is only relevant for the progression of patients who are susceptible, colonized or diseased. Unlike them, a patient who is resistant will remain resistant until and unless they receive an antibiotic at which time they become susceptible to colonization.

Susceptible patients and colonized patients who are not immunocompromised have their time since beginning antibiotic treatment updated. Colonized patients who are immunocompromised have their time until diseased updated. Three classes of diseased patients are considered here. Those who have been screened successfully but have not yet reached the turnaround time have their time since screening updated. The turnaround time for a screening is the time between administering the test and receiving the results. Those who have been screened unsuccessfully but have not yet reached the turnaround time also have their time since screening updated. In this way, they will not be screened again until at least the turnaround time has passed.

Finally, those who have been screened successfully and have begun treatment have their time since beginning treatment updated.

3.3.2 Admission

Each time step, a number of patients are admitted. This is referred to as an admission class. The same number of patients is admitted as were just discharged. This is done to assure consistency, so that the number of patients to be admitted does not exceed the number of vacant rooms. Moreover, the number of patients being discharged varies significantly each time step since it is ultimately based on the patients' varying lengths of stay and times since admission.

For each admission class, the probability of a patient being resistant upon admission is 0.58 while the probability of being diseased upon admission is 0.01 (Lanzas et al., 2011). However, for each admission class, at each time step, the probability of being susceptible upon admission is chosen randomly from a uniform distribution ranging from 0.21 to 0.40. This value will fix the corresponding probability of being colonized upon admission which will range between 0.01 and 0.20.

Each patient is randomly admitted to a vacant room and their time since admission is initialized. They are then assigned a disease status according to the above probabilities as well as a length of stay based on the hospital dataset. The procedure for this assignment is described in detail in Section 3.3.10.

Susceptible patients are given an antibiotic history since patients become susceptible to colonization via the disruption of the flora caused by antibiotic treatment. First, a particular type of antibiotic is assigned according to the treatment length, time until flora recovery, and the risk level vis à vis CDI associated with this antibiotic. This procedure is described in Section 3.3.7. Second, a time since beginning antibiotic treatment is assigned. This is a random integer drawn from a uniform distribution ranging from 0 to an upper limit defined as the sum of the treatment length (14

half-days) and time until flora recovery (28 half-days for low and high-risk antibiotic, 70 half-days for very high-risk antibiotic). That is, we regard a patient as susceptible to colonization from the moment they begin an antibiotic treatment and they can remain susceptible as long as their gut flora is not normal. Finally, the patient is assigned a time since becoming susceptible. In this case, it is precisely the time since they began antibiotic treatment.

Colonized patients either will or will not mount an immune response and so are characterized as one or the other according the global variable for the probability that a colonized patient is immunocompromised. Patients who are not immunocompromised are given an antibiotic history. First, an antibiotic is assigned in the same way as described above for susceptible patients. Second, a time since beginning antibiotic treatment is assigned; again, in the same way as for susceptible patients. Lastly, they are assigned a time since becoming colonized. A patient may have become colonized at any time since they began antibiotic treatment and, thus, this variable is assigned a uniform random integer between 0 and the time since they began treatment.

If the colonized patient is immunocompromised, they will become diseased at a certain point in time that must be assigned. First, an antibiotic history is assigned. In this case, what matters most is the risk level associated with their antibiotic assignment. Next, the length of the incubation period is determined. The incubation period depends on the risk level associated with their antibiotic assignment. For each level of antibiotic risk, there is a pair of global values for the minimum and maximum length of the incubation period. Baseline values for these pairs are (20,60), (14,40), and (8,20) for low, high, and very high risk antibiotics respectively. A random integer from a uniform distribution of integers in the appropriate range is assigned as the length of the incubation period. The patient's time until becoming diseased is assigned as a random integer greater than or equal to 0 but less than the incubation period. The time since current disease status in this case is equal to the length of the incubation period minus the time until becoming diseased.

Finally, for patients who are diseased upon admission, it is decided if the initial screening will be successful in identifying them as diseased according to the global variable for the sensitivity of the test and it is also decided if treatment will be successful according the global variable for this probability. The baseline values for the sensitivity and probability of successful treatment are 0.91 (Planche et al., 2008) and 0.8 (McFarland, 2008) respectively. Patients who will be identified as diseased due to successful screening are assigned a time since the successful screen. In this way, they will be identified when that time reaches the turnaround time for the test. The baseline value for the turnaround is 2 half-days (Planche et al., 2008). At that point the patient will be quarantined and treatment will begin as described in Section 3.3.9. Diseased patients who are unsuccessfully screened will not be tested again until after the turnaround time for the test and so are assigned a time since the unsuccessful screening.

3.3.3 Update Contamination Status

After a class of patients is admitted, the environment is updated. Each room has a contamination status of clean, contaminated, or very contaminated represented by the values 0, 1, and 2 respectively. During an update, the contamination status of a room occupied by a colonized patient is set to 1 while the contamination status of a room occupied by a diseased patient is set to 2. This value is affected by the cleaning procedure (Section 3.3.6).

The ward-level contamination is the sum of the contamination status values of all the rooms in the same ward. Since each ward has 35 rooms, each with a maximum contamination value of 2, this will be an integer between 0 and 70. This sum excludes the contamination values of those rooms that contain a quarantined patient. Thus, our model assumes that quarantine is 100% effective. This does not effect, however, the uncertain level of cleaning the room will receive upon the discharge of the quarantined patient. This value will be used in determining the probability that

a susceptible patient will become colonized (Section 3.3.8). While healthcare workers are not agents of this model, their effect as vectors for disease transmission is implicit in the fact that ward-level contamination levels contribute to patient colonization. That is, the probability that a susceptible patient in a particular ward room will become colonized depends in part on the contamination level of the entire ward. We regard a hospital ward a reasonable measure of the scope of a healthcare worker's interaction with patients. Therefore, the contamination level of the ward, rather than that of the individual patient room, contributes to the probability of becoming colonized.

3.3.4 Update Disease Status

Each half-day there is a probability that a patient will begin an antibiotic treatment-even if they are currently being treated with antibiotics. This model parameter was chosen so that simulation outputs pertaining to overall number of antibiotic treatments per patient reflect the hospital dataset. One of the model control strategies is to reduce the overall number of treatments by a certain proportion. This is implemented in the following way. Of all the patients that were assigned to receive a treatment each half day according to the probability just described, only a proportion of them will now actually receive a treatment.

The transitions described in this section are illustrated by the diagram in Figure 3.1. If a resistant patient goes on an antibiotic, they become susceptible and an antibiotic is assigned. The time since beginning antibiotic and time since current disease status are set to 0. A new length of stay is selected for this patient according the new disease status. If it is longer than the patient's current length of stay, then the patient's length of stay is changed to this value.

Each half-day, there is a probability that a susceptible patient will regain resistance. This probability is a logistic function of the time since they began their most recent antibiotic treatment. In particular, let t be the time since the patient

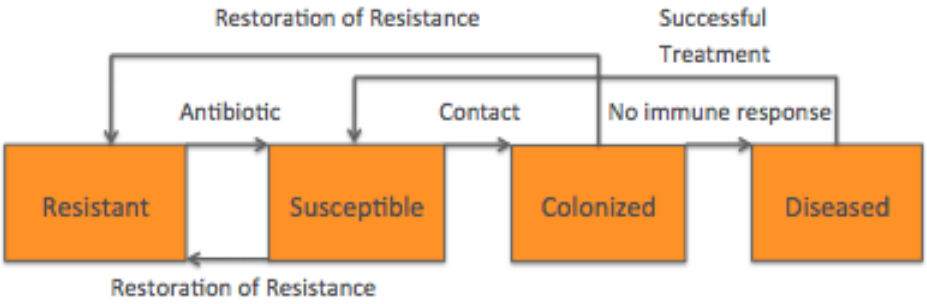

Figure 3.1: Disease state transitions for CDI

began antibiotic treatment and let T be the sum of the treatment length and the associated time until a normal flora is restored. Then, the probability, p, of regaining resistance is given by

$$p = \frac{1 - p_{min}}{1 + e^{-\left(\frac{12}{T}(t - \frac{T}{2})\right)}} + p_{min},$$

where $p_{min} = 0.2$ is the minimum probability of regaining resistance and the parameter value 12 determines the steepness of the logistic curve.

If they do not regain resistance, there is a probability they will receive an additional antibiotic as described above. Then, there is a probability they will become colonized (Section 3.3.8). If they do become colonized, they are designated as either immunocompromised or not according to the global variable for the probability of being immunocompromised. If the now colonized patient is immunocompromised, then an incubation period is assigned as before. This value determines when they will become diseased. Furthermore, the number of nosocomial colonizations is tracked.

Similar to susceptible patients, colonized patients who will mount an immune response can regain resistance. If they do not regain resistance, there is a chance they will receive an additional antibiotic; this is also the case for those patients who will not mount an immune response. For these patients, if their incubation period is over, they become diseased. If that happens, they will be screened at the next time step (because they are now symptomatic) and it is determined if the screening will be successful in identifying them as diseased according to the global variable for

sensitivity. It is also decided if the subsequent treatment will be successful according the global variable for this probability. The number of nosocomial diseases is tracked.

A diseased patient is quarantined and treatment is begun (Section 3.3.9) if they have been identified; that is, if they were successfully screened and they have reached the turnaround time. A diseased patient who has not been identified as diseased is re-screened if the turnover time since the unsuccessful screening has been reached. Diseased patients that have completed a successful treatment become susceptible.

3.3.5 Discharge Patients

Patients are discharged if their length-of-stay variable is the same value as their time-since-admission variable. The current disease status, disease status at admission and the number of antibiotics received during their stay are tallied for each discharged patient.

3.3.6 Cleaning

After a patient is discharged, the vacant room is cleaned. If the room has contamination status 2 or 1, then there is a probability that cleaning will result in a new contamination status of 1 or 0, respectively. The probability of effective cleaning is a global variable. A baseline value of 0.5 was assigned to this variable under the simple assumption that different cleaning measures could be more or less effective at reducing the level of contamination.

3.3.7 Antibiotic Assignment

When a patient goes on an antibiotic, there is a probability that it will be low, high, or very high-risk with respect to CDI. There is a treatment length and time to normal flora associated with each class. The risk level is one factor in determining the probability of being colonized.

3.3.8 Assign Probability of Becoming Colonized

The half-daily probability of a susceptible patient becoming colonized depends on both the local, ward-level environment and the risk level associated with the antibiotic they are receiving.

The environment is classified as low, medium, or high contamination. These classifications are determined by the typical range and variance of ward-level contamination values for the simulations of this model.

The probabilities associated with different antibiotic risk levels (see Section 3.3.7) are determined using odds ratios. The odds ratio (OR) of interest in this case is a measure of the association between an exposure to antibiotic treatment and the outcome of becoming colonized by *C. difficile*. Studies have identified the odds ratios for colonization risk assigned to specific antibiotics (Bignardi, 1998; Feazel et al., 2014; Slimings and Riley, 2014). In our model, the OR represents the odds that a patient will become colonized if they have been given a high or very high risk antibiotic, compared to the odds of becoming colonized when given a low risk antibiotic. These are global variables in the model.

Let p be the half-daily probability of a susceptible patient becoming colonized given that they are being treated with a low risk antibiotic. In general, we can use p together with a known odds ratio value associated with a particular antibiotic to find the half daily probability of the patient becoming colonized given they are being treated with that particular antibiotic. Let OR_A be the odds ratio associated with antibiotic A and let p_A be the half daily probability of the patient becoming colonized given they are being treated with antibiotic A. Then the relationship

$$OR_A = \frac{p_A}{1-p_A} \Big/ \frac{p}{1-p},$$

implies

$$p_A = \frac{OR_A \cdot p}{1-p+OR_A \cdot p}.$$

Odds ratio values for the categories "high risk" and "very-high risk" are based on the odds ratio values for the individual antibiotics in these categories (Bignardi, 1998; Feazel et al., 2014; Slimings and Riley, 2014) as well as information from the hospital dataset regarding the relative proportion of the number of treatments for each specific antibiotic to the overall number of antibiotic treatments. For each category, a weighted average was calculated using the odds ratio values for each specific antibiotic in the category and the corresponding number of these treatments from the hospital dataset. In this way, we estimated the odds ratio values for high and very-high risk antibiotics to be $OR_h = 4$ and $OR_{vh} = 8$, respectively.

Since there is also an environmental component to colonization, we will have half-daily probabilities for each of the 9 combinations from the 3 environmental contamination levels and the 3 antibiotic risk categories; see Table 3.3. Let p_ℓ^h be the half-daily probability of a susceptible patient becoming colonized given that they are being treated with a low risk antibiotic in a highly contaminated environment. Here the subscript, ℓ, refers to the risk level associated with the antibiotic and stands for "low". The superscript, h, refers to the level of ward contamination and stands for "high". Table 3.3 indicates the values for each of the 9 combinations and how they are calculated.

First a value is assigned to p_ℓ^h. The value 0.15 for p_ℓ^h was chosen by calibration to match the proportion of nosocomial colonizations from the data. From this value and the values for OR_h and OR_{vh}, we calculate the other two probabilities for a highly contaminated environment, p_h^h and p_{vh}^h. Next, we calculate the probability, p_ℓ^ℓ, of a susceptible patient becoming colonized given that they are being treated with a low risk antibiotic in a low contamination environment. We do this by scaling down by a certain factor, q: $p_\ell^\ell = q \cdot p_\ell^h$. This factor is a measure of the relative contribution of the environment to the colonization of a susceptible patient. For the simulations we assigned the value 0.5 to the factor q. The other two probabilities for a low contamination environment are then calculated similar to above. Finally, we take p_ℓ^m

Table 3.3: Global variables for the half-daily probabilities of becoming colonized.

Variable	Antibiotic risk	Level of contamination	Value
p_ℓ^h	Low	High	$p_\ell^h = 0.15$
p_h^h	High	High	$OR_h \cdot p_\ell^h \Big/ \left(1 - p_\ell^h + OR_h \cdot p_\ell^h\right)$
p_{vh}^h	Very high	High	$OR_{vh} \cdot p_\ell^h \Big/ \left(1 - p_\ell^h + OR_{vh} \cdot p_\ell^h\right)$
p_ℓ^ℓ	Low	Low	$q \cdot p_\ell^h = 0.5 \cdot 0.15$
p_h^ℓ	High	Low	$OR_h \cdot p_\ell^\ell \Big/ \left(1 - p_\ell^\ell + OR_h \cdot p_\ell^\ell\right)$
p_{vh}^ℓ	Very high	Low	$OR_{vh} \cdot p_\ell^\ell \Big/ \left(1 - p_\ell^\ell + OR_{vh} \cdot p_\ell^\ell\right)$
p_ℓ^m	Low	Medium	$(p_\ell^h + p_\ell^\ell)/2$
p_h^m	High	Medium	$OR_h \cdot p_\ell^m \Big/ \left(1 - p_\ell^m + OR_h \cdot p_\ell^m\right)$
p_{vh}^m	Very high	Medium	$OR_{vh} \cdot p_\ell^m \Big/ \left(1 - p_\ell^m + OR_{vh} \cdot p_\ell^m\right)$

to be the average of p_ℓ^ℓ and p_ℓ^h and from this calculate the other two probabilities for a medium contamination environment.

3.3.9 Quarantine and Treat

In this model, quarantined means that the contamination level of their room does not contribute to the overall ward-level contamination. This models the effect of isolation and contact precautions that decrease the environmental bioburden associated with diarrhea (Gerding et al., 2008). When a patient is quarantined due to CDI, they begin treatment for CDI. This means they will be assigned an antibiotic (Section 3.3.7) and the time since beginning treatment is initialized.

3.3.10 Length of Stay

Patients are assigned a length of stay upon admission according to their disease status. This half-daily value is assigned by resampling summary data from the hospital dataset. In particular, given a patient's disease status, their length of stay is assigned by resampling from the relevant histogram generated by the length of stay data for patients with that disease status. The range of the values for the length of stay in half-days for resistant, susceptible, and diseased patients are $[0, 32], [0, 68]$

and $[0, 160]$, respectively. The range for colonized patients is the same as that for susceptible patients.

3.4 Control Strategies

The control measures considered in this study are antimicrobial stewardship and decontamination by cleaning. There are two basic strategies employed in the implementation of an antimicrobial stewardship program.

One strategy is to reduce the overall number of antibiotic prescriptions by some proportion. Here we consider three values for such reduction, $0, 0.1$, and 0.2, where no reduction is considered the baseline value. Let q_r be the reduction proportion. This reduction is achieved in the model by first deciding whether a patient would receive an antibiotic according to the global variable prob-antib with value 0.27 (Table 3.2), and then, if they were to receive one in the situation with no reduction, there is now a probability of $1 - q_r$ that they will receive an antibiotic.

Alternatively, rather than reducing the number of prescriptions, the relative proportions of antibiotics prescribed by *type* are changed. In particular, we are interested in differentiating antibiotics by the level of CDI risk with which they are associated. As described in Section 3.3.7, there are three categories of risk in this model, 'low', 'high', and 'very high.' We consider three scenarios. The baseline scenario, established from the hospital dataset, has the proportions $0.4, 0.26$, and 0.34 for 'low', 'high', and 'very high' respectively. For a second scenario, we consider replacing half of the very high risk prescriptions with high risk antibiotics. The corresponding proportions for this scenario are $0.4, 0.43$, and 0.17. Finally, in addition to replacing half of the very high risk prescriptions with high risk antibiotics, we also replace half of the high risk prescriptions with low risk antibiotics. The resulting proportions for this scenario are $0.53, 0.3$, and 0.17. These scenarios are summarized in Table 3.4.

Table 3.4: Antibiotic risk proportion scenarios.

Scenario	Proportion low-risk	Proportion high-risk	Proportion very high-risk
1	0.4	0.26	0.34
2	0.4	0.43	0.17
3	0.53	0.3	0.17

As described in Section 3.3.6, there is a global variable in the model assigning a probability of effective cleaning. We select three values for this variable to represent the effect of certain levels of the effectiveness of a cleaning *strategy*. A baseline value of 0.5 was assigned to this variable under the simple assumption that different cleaning measures could be more or less effective at reducing the level of contamination. Accordingly, the other two values considered are 0.2 and 0.8.

3.5 Simulation Results for Stewardship Strategies

A complete factorial design for the combination of these three strategies with each of their respective three scenarios was implemented. The 27 strategies are summarized in Table 3.5. One hundred runs were completed for each strategy. In the figures to follow, the combination strategy will be referred to by its corresponding number in this table. Note that combination strategy number 2 is the baseline scenario. Recall that the baseline scenario is the scenario that corresponds to the data set used to design the model (see Section 3.2.2) and reflects current strategies for controlling disease transmission. Strategy number 2 reflects no reduction in the number of antibiotic treatments given and, so, the baseline value for the proportion reduction is 0. The relative proportions of treatments from the hospital dataset that were low, high, and very-high risk with respect to CDI are $0.4, 0.26$ and 0.34 respectively. These are, therefore, the baseline risk-scenario. Finally, as described above, the baseline value for effective cleaning, 0.5 was chosen in order to compare strategies that are both more effective and less effective in this regard.

Table 3.5: Numbering of combination strategies.

Combination	Proportion reduction	Risk-scenario	Probability of effective cleaning
1	0	1	0.2
2	0	1	0.5
3	0	1	0.8
4	0	2	0.2
5	0	2	0.5
6	0	2	0.8
7	0	3	0.2
8	0	3	0.5
9	0	3	0.8
10	0.1	1	0.2
11	0.1	1	0.5
12	0.1	1	0.8
13	0.1	2	0.2
14	0.1	2	0.5
15	0.1	2	0.8
16	0.1	3	0.2
17	0.1	3	0.5
18	0.1	3	0.8
19	0.2	1	0.2
20	0.2	1	0.5
21	0.2	1	0.8
22	0.2	2	0.2
23	0.2	2	0.5
24	0.2	2	0.8
25	0.2	3	0.2
26	0.2	3	0.5
27	0.2	3	0.8

The outputs to measure the relative effectiveness of these strategies were the incidence numbers of nosocomial colonizations and diseases per year, while the total number of admissions per year is 10,458 on average. In the box plots shown in Figure 3.2, the 27 combined strategies are ranked according to their respective median values of nosocomial colonizations. These median values are indicated by the circles with dots in the center. The top chart contains box plots for the number of new colonizations by strategy and they are plotted in increasing order by median values. The bottom chart indicates the corresponding box plots for the number of new diseases.

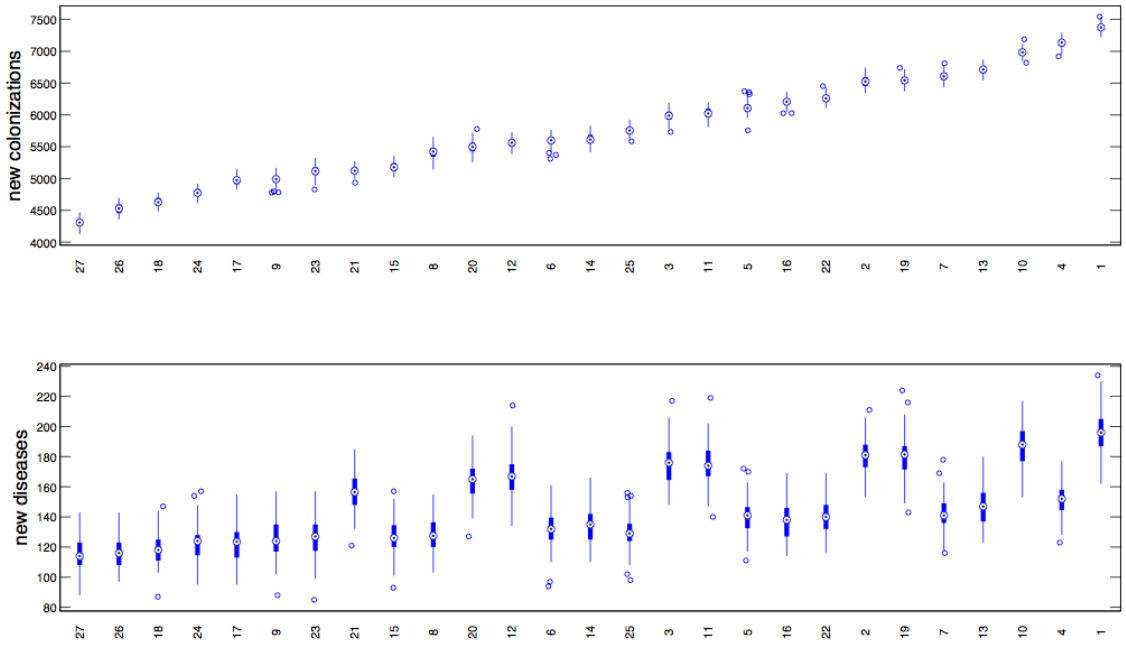

Figure 3.2: Box plots for strategies ranked by number of new colonizations at top and corresponding box plots for number of new diseases on bottom

Note, for example, the rank of the baseline scenario, scenario 2. There are 6 scenarios that, on average, resulted in more new colonizations. As one would expect, each of these 6 scenarios $(19, 7, 13, 10, 4, 1)$ are cases where the probability of effective cleaning is less than the baseline value for this probability. Recall that the baseline value for this probability is 0.5 and in the 6 scenarios it is 0.2. It is worth pointing out, however, that there are 3 scenarios $(16, 22, 25)$ with probability 0.2 of effective cleaning that, on average, resulted in *fewer* new colonizations. For scenario 22, the median number of new colonizations is 6261 which is 4% less than the 6525 colonizations for the baseline scenario. Scenario 16 results in 5% fewer colonizations. In scenario 25, however, the median number of new colonizations was 5756 compared to the baseline median value of 6525, which is a 12% reduction. The strategy implemented in scenario 25 involved both a reduction in overall antibiotic treatments as well as a reduction in the relative proportions of antibiotic treatments that are high and very-high risk with respect to CDI. This suggests that it is possible for an aggressive antibiotic

stewardship strategy reduce the number of new colonizations even in the event of less effective cleaning.

The bottom chart in Figure 3.2 shows the corresponding numbers of nosocomial diseases. These numbers do not necessarily increase respectively by scenario to the numbers of new colonizations. As noted above, compared to the baseline scenario, the reduction in new colonizations for scenario 22 was modest compared to that for scenario 25: 4% compared to 12%. The corresponding comparison of these scenarios for the reduction in new diseases is much closer: 23% compared to 29%. The only difference between these two strategies is that scenario 22 represents risk-scenario number 2 while scenario 25 represents risk-scenario number 3 (see Table 3.4). This suggests that there are strategies that may be similarly effective with respect to reducing the number of nosocomial colonizations but differ significantly in terms of reducing nosocomial diseases.

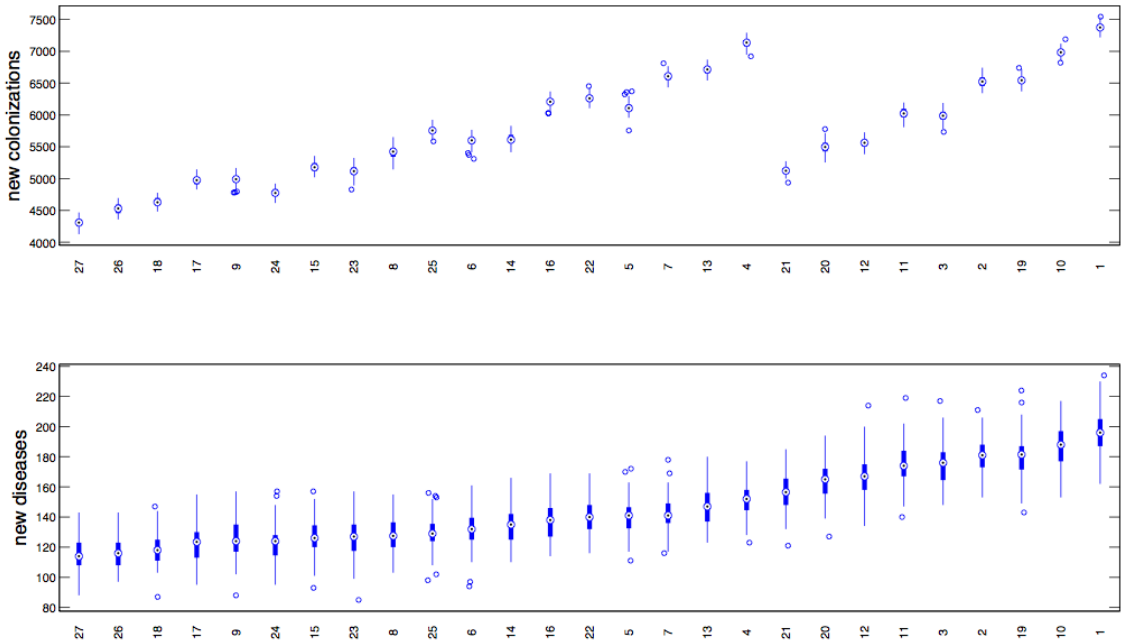

Figure 3.3: Box plots for strategies ranked by number of new diseases on bottom and corresponding box plots for number of new colonizations on top

In Figure 3.3, the 27 combined strategies are ranked according to their respective median values of nosocomial diseases. The bottom chart contains box plots for the

number of new diseases by strategy and they are plotted in increasing order by median values. The top chart indicates the corresponding box plots for the number of new colonizations. By this ranking there are only 3 scenarios that, on average, resulted in more new diseases than the baseline scenario. And, again, each of these 3 are scenarios where the probability of effective cleaning is less than that of the baseline scenario. There are, therefore, 6 scenarios in which the probability of effective cleaning is less than that of the baseline scenario and, yet, are more effective in reducing the number of new diseases. Of these, scenario 25 represents the largest reduction and was discussed above as having 29% less disease incidence than the baseline scenario.

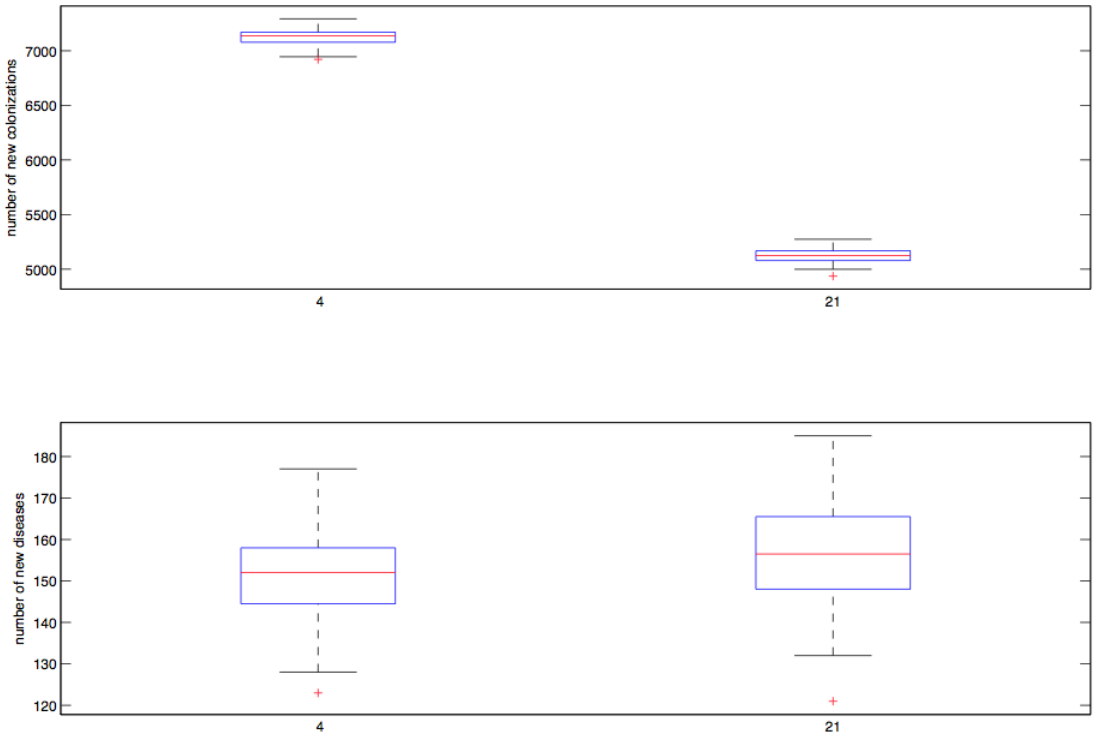

Figure 3.4: Box plots for strategies 4 and 21 for numbers of new colonizations on top and new diseases on bottom

What stands out when ranked according to the number of new diseases is the corresponding change in the number of new colonizations. In particular, we note a significant change in the number of new colonizations between scenarios 4 and 21 (see Figure 3.4). The median numbers of new diseases for these two scenarios are

close to the same, 152 and 157 respectively. The median number, 7137, of new colonizations represented by scenario 4 is, however, 39% more than the 5124 new colonizations represented by scenario 21. The strategy for scenario 4 involves no reduction in the overall proportion of antibiotic treatments but it does represent stewardship of the relative proportions of treatments according to risk using risk scenario 2 (see Table 3.4). Scenario 21, on the other hand, does not implement a stewardship of risk proportions, but, rather, it implements an overall reduction in the number of treatments and a more effective cleaning strategy. This suggests that there are strategies that may be similarly effective with respect to reducing the number of nosocomial diseases but differ significantly in terms of reducing nosocomial colonizations. In terms of policy, it is important to consider strategies the efficacy of which are evaluated in terms of reducing both nosocomial diseases and colonizations. One important consequence of ignoring the reduction of nosocomial colonizations is that many of these individuals will develop the disease after leaving the hospital. This will inevitably lead to an increase in the admission rate of diseased patients (Otten et al., 2010).

Suppose one wants to implement only one of the three strategies and wants to know the relative efficacy of one strategy over another in reducing nosocomial colonizations and/or diseases. Table 3.6 summarizes the relevant values from our simulations for making this evaluation. From this perspective, the best *single* strategy to implement is one that reduces both the relative proportion of antibiotic treatments that are high risk with respect to CDI and the relative proportion of antibiotic treatments that are very-high risk with respect to CDI. Table 3.6 indicates that this strategy does the best in terms of reducing nosocomial colonizations and it also does the best in terms of reducing nosocomial diseases. The median number of new colonizations for this strategy is 5424 which is 17% less than the baseline number of new colonizations which is 6525. The median number of new diseases for this strategy is 128 which is 29% less than the baseline number of new diseases which is 181. In fact, in terms of reducing nosocomial diseases, the other strategy in this category ranks 2^{nd}, with 141

new diseases which is 22% less than the baseline. This is the strategy that reduces the relative proportion of antibiotic treatments that are very-high risk with respect to CDI but does not reduce the relative proportion of antibiotic treatments that are high risk with respect to CDI. If the more aggressive strategy is unrealizable or, perhaps, too expensive, then one might choose the same type of, but less aggressive, stewardship policy. This would be, however, another example of ignoring the value of reducing the number of nosocomial colonizations. Notice that this strategy, while ranking 2^{nd} with respect to reducing the number of diseases, ranks 5^{th} with respect to reducing the number of colonizations; only slightly better than the baseline scenario. Once again, it is important for policies to consider strategies that are effective in reducing both nosocomial diseases and colonizations. If one wishes to take into account both goals (and the more aggressive strategy is not available), then the next best strategy is the *other* type of stewardship policy that reduces the overall number of treatments by 20%. This highlights the importance of understanding the complexities of *Clostridium difficile* transmission in order to make the best decisions with respect to implementing control measures.

Table 3.6: Median colonizations and diseases for employing a single strategy

Parameter to vary	Parameter value	Median colonizations	Median diseases	Rank by colonizations	Rank by diseases
Probability of	0.2	7376	196	7	7
effective cleaning	0.8	5988	176	3	5
Risk-scenario	2	6109	141	5	2
Table 3.4	3	5424	128	1	1
Proportion	0.1	6024	174	4	4
reduction	0.2	5498	165	2	3
	Baseline:	6525	181	6	6

3.6 Conclusions

In this study we have pointed out the significance to nosocomial transmission of *Clostridium difficile* of important sources, including the role of asymptomatic

carriers, environmental heterogeneity, and the complex role of antibiotic treatments in hospitals.

We implemented an ABM for *Clostridium difficile* transmission in hospitals that accounts for several processes and individual factors including environmental and antibiotic heterogeneity in order to evaluate the efficacy of various control measures aimed at reducing environmental contamination and mitigating the effects of antibiotic use on transmission. In particular, we accounted for local contamination levels in our ABM which contribute to the probability of colonization. These levels are influenced in our model by the probability of effective cleaning and, so, served as a control for modeling environmental decontamination. We also accounted for both the number and type of antibiotic treatments given to patients in our model and, so, served as controls for modeling antimicrobial stewardship.

Our model showed that it is possible for an aggressive antibiotic stewardship strategy to reduce the number of new colonizations even in the event of less effective cleaning. We showed that there are strategies that may be similarly effective with respect to reducing the number of nosocomial colonizations but differ significantly in terms of reducing nosocomial diseases. We showed that there are, likewise, strategies that may be similarly effective with respect to reducing the number of nosocomial diseases but differ significantly in terms of reducing nosocomial colonizations.

In an evidence-based systematic review, Hsu et al. (2010), seek to identify and critically evaluate the efficacy of interventions for the prevention of CDI in healthcare institutions. Corroborating our modeling results, this study concludes that there is good evidence to support the effectiveness of antimicrobial stewardship for preventing healthcare-associated CDI. While this study does address, for example, the ineffectiveness of treating asymptomatic carriers for preventing healthcare-associated CDI, it does not consider the *prevention* of colonization as an important metric for making such an evaluation. Our modeling study suggests, however, that it is important for policy makers to consider strategies that are effective in reducing both nosocomial diseases and colonizations. An important consequence of ignoring the

reduction of nosocomial colonizations is that many of these individuals will develop the disease after leaving the hospital which, in turn, can lead to an increase in the admission rate of diseased patients. We have shown, therefore, the importance of not evaluating the efficacy of a strategy based solely on its success in reducing nosocomial diseases.

We also considered the situation wherein one implements only one of the three strategies for the control of *Clostridium difficile* transmission. We showed the relative efficacy of one strategy over another in reducing nosocomial colonizations and/or diseases. Another example illustrates that choosing a strategy for the goal of reducing nosocomial diseases does not necessarily achieve the the same relative success for the goal of reducing nosocomial colonizations. This is an important oversight since discharging more patients who are colonized by *Clostridium difficile* will lead to more individuals that develop the disease after leaving the hospital. This will inevitably lead to an increase in the admission rate of diseased patients.

The agent-based model presented here is a useful tool for investigating strategies for reducing the overall *Clostridium difficile* burden in healthcare settings. In the future, we plan to design simulations for evaluating management strategies that are connected to current practices in order to predict their expected impact on *Clostridium difficile* burden. For example, an aggressive antimicrobial stewardship policy may be difficult to implement and will likely be influenced by both the needs of patients and the actual pathogens involved. Our model can easily incorporate the compliance habits of healthcare workers and can be adapted to other hospital datasets and management protocols.

Bibliography

Bartlett, J. G. (2002). Antibiotic-associated diarrhea. *New England Journal of Medicine*, 346(5):334–339. 6, 61

Belgacem, F. and Cosner, C. (1995). The effects of dispersal along environmental gradients on the dynamics of populations in heterogeneous environments. *Canad. Appl. Math. Quart.*, 3(4):379–397. 9

Bignardi, G. (1998). Risk factors for *Clostridium difficile* infection. *Journal of Hospital Infection*, 40(1):1 – 15. The 4th International Conference of the Hospital Infection Society Effective Infection Control: Ahead of Change. 79, 80

Brauer, F. (2015). Some simple nosocomial disease transmission models. *Bulletin of Mathematical Biology*, 77(3):460–469. 62

Brézis, H. (2010). *Functional Analysis, Sobolev Spaces and Partial Differential Equations*. Universitext Series. Springer. 24

Cantrell, R. and Cosner, C. (1991a). The effects of spatial heterogeneity in population dynamics. *Journal of Mathematical Biology*, 29(4):315–338. 3, 9

Cantrell, R. S. and Cosner, C. (1989). Diffusive logistic equations with indefinite weights: population models in disrupted environments. *Proc. Roy. Soc. Edinburgh Sect. A*, 112(3-4):293–318. 3, 9

Cantrell, R. S. and Cosner, C. (1991b). Diffusive logistic equations with indefinite weights: population models in disrupted environments. II. *SIAM J. Math. Anal.*, 22(4):1043–1064. 3, 9

Cantrell, R. S. and Cosner, C. (2003). *Spatial ecology via reaction-diffusion equations*. Wiley Series in Mathematical and Computational Biology. John Wiley & Sons, Ltd., Chichester. 8

Cantrell, R. S., Cosner, C., and Lou, Y. (2008). Approximating the ideal free distribution via reaction-diffusion-advection equations. *J. Differential Equations*, 245(12):3687–3703. 9

Cantrell, S., Cosner, C., and Ruan, S. (2009). *Spatial Ecology*. Chapman & Hall/CRC Mathematical and Computational Biology. Taylor & Francis. 8

Codella, J., Safdar, N., Heffernan, R., and Alagoz, O. (2015). An agent-based simulation model for *Clostridium difficile* infection control. *Medical Decision Making*, 35(2):211–229. 64

Cohen, Stuart H., M., Gerding, Dale N., M., Stuart Johnson, M., Kelly, Ciaran P., M., Loo, Vivian G., M., McDonald, L. Clifford, M., Pepin, Jacques, M., and Wilcox, Mark H., M. (2010). Clinical practice guidelines for *Clostridium difficile* infection in adults: 2010 Update by the Society for Healthcare Epidemiology of America (SHEA) and the Infectious Diseases Society of America (IDSA). *Infection Control and Hospital Epidemiology*, 31(5):pp. 431–455. 6, 62

Cosner, C. and Lou, Y. (2003). Does movement toward better environments always benefit a population? *J. Math. Anal. Appl.*, 277(2):489–503. 9

Curry, S. R., Muto, C. A., Schlackman, J. L., Pasculle, A. W., Shutt, K. A., Marsh, J. W., and Harrison, L. H. (2013). Use of multilocus variable number of tandem repeats analysis genotyping to determine the role of asymptomatic carriers in *Clostridium difficile* transmission. *Clinical Infectious Diseases*, 57(8):1094–1102. 64

D'Agata, E. M., Magal, P., Olivier, D., Ruan, S., and Webb, G. F. (2007). Modeling antibiotic resistance in hospitals: The impact of minimizing treatment duration. *Journal of Theoretical Biology*, 249(3):487 – 499. 64

Dancer, S., Kirkpatrick, P., Corcoran, D., Christison, F., Farmer, D., and Robertson, C. (2013). Approaching zero: temporal effects of a restrictive antibiotic policy on

hospital-acquired *Clostridium difficile*, extended-spectrum β-lactamase-producing coliforms and meticillin-resistant *Staphylococcus aureus*. *International Journal of Antimicrobial Agents*, 41(2):137 – 142. 7, 63, 64, 65

Ding, W., Finotti, H., Lenhart, S., Lou, Y., and Ye, Q. (2010). Optimal control of growth coefficient on a steady-state population model. *Nonlinear Analysis: Real World Applications*, 11(2):688 – 704. 10

Donskey, C. J. (2010). Preventing transmission of *Clostridium difficile*: Is the answer blowing in the wind? *Clinical Infectious Diseases*, 50(11):1458–1461. 63

Dubberke, E. R. and Olsen, M. A. (2012). Burden of *Clostridium difficile* on the healthcare system. *Clinical Infectious Diseases*, 55(suppl 2):S88–S92. 6, 62

Dubberke, Erik R., M., Dale N. Gerding, M., David Classen, MD, M., Kathleen M. Arias, MS, C., Kelly Podgorny, RN, M. C., Deverick J. Anderson, MD, M., Helen Burstin, M., David P. Calfee, MD, M., Susan E. Coffin, MD, M., Victoria Fraser, M., Frances A. Griffin, RRT, M., Peter Gross, M., Keith S. Kaye, M., Michael Klompas, M., Evelyn Lo, M., Jonas Marschall, M., Leonard A. Mermel, DO, S., Lindsay Nicolle, M., David A. Pegues, M., Trish M. Perl, M., Sanjay Saint, M., Cassandra D. Salgado, MD, M., Robert A. Weinstein, M., Robert Wise, M., and Deborah S. Yokoe, MD, M. (2008). Strategies to prevent *Clostridium difficile* infections in acute care hospitals. *Infection Control and Hospital Epidemiology*, 29(S1):pp. S81–S92. 6, 62, 63

Dubberke, Erik R., M. M., Carling, Philip, M., Carrico, Ruth, P. R., Donskey, Curtis J., M., Loo, Vivian G., M. M., McDonald, L. Clifford, M., Maragakis, Lisa L., M. M., Sandora, Thomas J., M. M., Weber, David J., M. M., Yokoe, Deborah S., M. M., and Gerding, Dale N., M. (2014). Strategies to prevent *Clostridium difficile* infections in acute care hospitals: 2014 update. *Infection Control and Hospital Epidemiology*, 35(6):pp. 628–645. 6, 62, 63

Evans, L. C. (2010). *Partial differential equations*, volume 19 of *Graduate Studies in Mathematics*. American Mathematical Society, Providence, RI, second edition. 19, 29, 31

Feazel, L. M., Malhotra, A., Perencevich, E. N., Kaboli, P., Diekema, D. J., and Schweizer, M. L. (2014). Effect of antibiotic stewardship programmes on *Clostridium difficile* incidence: a systematic review and meta-analysis. *Journal of Antimicrobial Chemotherapy*, 69(7):1748–1754. 7, 63, 64, 65, 79, 80

Fister, K. (1997). Optimal control of harvesting in a predator-prey parabolic system. *Houston Journal of Mathematics*, 23(2):341–355. 41

Fister, K. (2001). Optimal control of harvesting coupled with boundary control in a predatorprey system. *Applicable Analysis: An International Journal*, 77(1-2):11–28. 41

Gerding, D. N., Muto, C. A., and Owens, R. C. (2008). Measures to control and prevent *Clostridium difficile* infection. *Clinical Infectious Diseases*, 46(Supplement 1):S43–S49. 6, 63, 65, 67, 81

Grimm, V., Berger, U., DeAngelis, D. L., Polhill, J. G., Giske, J., and Railsback, S. F. (2010). The ODD protocol: A review and first update. *Ecological Modelling*, 221(23):2760 – 2768. 66

Hackbusch, W. (1978). A numerical method for solving parabolic equations with opposite orientations. *Computing*, 20(3):229–240. 46

Holmes, E. E., Lewis, M. A., Banks, J. E., and Veit, R. R. (1994). Partial differential equations in ecology: Spatial interactions and population dynamics. *Ecology*, 75(1):pp. 17–29. 8

Hsieh, Y.-H., Liu, J., Tzeng, Y.-H., and Wu, J. (2014). Impact of visitors and hospital staff on nosocomial transmission and spread to community. *Journal of Theoretical Biology*, 356(0):20 – 29. 62

Hsu, J., Abad, C., Dinh, M., and Safdar, N. (2010). Prevention of endemic healthcare-associated *Clostridium difficile* infection: Reviewing the evidence. *The American Journal of Gastroenterology*, 105(11):2327–2339. 65, 90

Kareiva, P., Mullen, A., and Southwood, R. (1990). Population dynamics in spatially complex environments: Theory and data. *Philosophical Transactions of the Royal Society of London B: Biological Sciences*, 330(1257):175–190. 8

Krylov, N. (1987). *Nonlinear Elliptic and Parabolic Equations of the Second Order*. Mathematics and its Applications. Springer Netherlands. 19, 20

Lanzas, C., Dubberke, E. R., Lu, Z., Reske, K. A., and Grohn, Y. (2011). Epidemiological model for *Clostridium difficile* transmission in healthcare settings. *Infection Control*, 32(06):553–561. 7, 62, 66, 73

Lanzas, Cristina, P. and Dubberke, Erik R., M. (2014). Effectiveness of screening hospital admissions to detect asymptomatic carriers of *Clostridium difficile*: A modeling evaluation. *Infection Control and Hospital Epidemiology*, 35(8):pp. 1043–1050. 62

Leffler, D. A. and Lamont, J. T. (2015). *Clostridium difficile* infection. *New England Journal of Medicine*, 372(16):1539–1548. PMID: 25875259. 61

Lenhart, S., Liang, M., and Protopopescu, V. (1999). Optimal control of boundary habitat hostility for interacting species. *Mathematical Methods in the Applied Sciences*, 22(13):1061–1077. 41

Lenhart, S. and Workman, J. (2007). *Optimal Control Applied to Biological Models*. Chapman & Hall/CRC Mathematical and Computational Biology. Taylor & Francis. 46

Lessa, F. C., Mu, Y., Bamberg, W. M., Beldavs, Z. G., Dumyati, G. K., Dunn, J. R., Farley, M. M., Holzbauer, S. M., Meek, J. I., Phipps, E. C., Wilson, L. E., Winston,

L. G., Cohen, J. A., Limbago, B. M., Fridkin, S. K., Gerding, D. N., and McDonald, L. C. (2015). Burden of *Clostridium difficile* infection in the United States. *New England Journal of Medicine*, 372(9):825–834. PMID: 25714160. 61, 62

LeVeque, R. (2007). *Finite Difference Methods for Ordinary and Partial Differential Equations*. Society for Industrial and Applied Mathematics. 47

Li, X. J. and Yong, J. M. (1995). *Optimal control theory for infinite-dimensional systems*. Systems & Control: Foundations & Applications. Birkhäuser Boston, Inc., Boston, MA. 2, 11

Lions, J.-L. (1971). *Optimal control of systems governed by partial differential equations.* Translated from the French by S. K. Mitter. Die Grundlehren der mathematischen Wissenschaften, Band 170. Springer-Verlag, New York-Berlin. 2, 11

Lions, J.-L. (1972). *Some aspects of the optimal control of distributed parameter systems*. Society for Industrial and Applied Mathematics, Philadelphia, Pa. Conference Board of the Mathematical Sciences Regional Conference Series in Applied Mathematics, No. 6. 2, 11

Lou, Y. (2006). On the effects of migration and spatial heterogeneity on single and multiple species. *J. Differential Equations*, 223(2):400–426. 8

McFarland, L. V. (2008). Update on the changing epidemiology of *Clostridium difficile*-associated disease. *Nature Clinical Practice Gastroenterology & Hepatology*, 5(1):40–48. 75

McMaster-Baxter, N. L. and Musher, D. M. (2007). *Clostridium difficile*: Recent epidemiologic findings and advances in therapy. *Pharmacotherapy: The Journal of Human Pharmacology and Drug Therapy*, 27(7):1029–1039. 63

Murray, J. and Sperb, R. (1983). Minimum domains for spatial patterns in a class of reaction diffusion equations. *Journal of Mathematical Biology*, 18(2):169–184. 9

Murray, J. D. (2003). *Mathematical biology. II*, volume 18 of *Interdisciplinary Applied Mathematics*. Springer-Verlag, New York, third edition. Spatial models and biomedical applications. 8

Neilan, R. M. and Lenhart, S. (2011). Optimal vaccine distribution in a spatiotemporal epidemic model with an application to rabies and raccoons. *Journal of Mathematical Analysis and Applications*, 378(2):603 – 619. 41

Okubo, A. and Levin, S. A. (2001). *Diffusion and ecological problems: modern perspectives*, volume 14 of *Interdisciplinary Applied Mathematics*. Springer-Verlag, New York, second edition. 8

Otten, A. M., REID-SMITH, R. J., FAZIL, A., and WEESE, J. S. (2010). Disease transmission model for community-associated *Clostridium difficile* infection. *Epidemiology & Infection*, 138:907–914. 88

Planche, T., Aghaizu, A., Holliman, R., Riley, P., Poloniecki, J., Breathnach, A., and Krishna, S. (2008). Diagnosis of *Clostridium difficile* infection by toxin detection kits: a systematic review. *The Lancet Infectious Diseases*, 8(12):777 – 784. 70, 75

Pontryagin, L. S., Boltyanskii, V. G., Gamkrelidze, R. V., and Mishchenko, E. F. (1962). *The mathematical theory of optimal processes*. Translated from the Russian by K. N. Trirogoff; edited by L. W. Neustadt. Interscience Publishers John Wiley & Sons, Inc. New York-London. 1, 10

Rubin, M. A., Jones, M., Leecaster, M., Khader, K., Ray, W., Huttner, A., Huttner, B., Toth, D., Sablay, T., Borotkanics, R. J., Gerding, D. N., and Samore, M. H. (2013). A simulation-based assessment of strategies to control *Clostridium difficile* transmission and infection. *PLoS ONE*, 8(11):e80671. 64

Rupnik, M., Wilcox, M. H., and Gerding, D. N. (2009). *Clostridium difficile* infection: new developments in epidemiology and pathogenesis. *Nature Reviews Microbiology*, 7(7):526–536. 63

Simon, J. (1987). Compact sets in the space $L^p(0,T;B)$. *Ann. Mat. Pura Appl. (4)*, 146:65–96. 22

Skellam, J. G. (1951). Random dispersal in theoretical populations. *Biometrika*, 38:196–218. 8

Slimings, C. and Riley, T. V. (2014). Antibiotics and hospital-acquired *Clostridium difficile* infection: update of systematic review and meta-analysis. *Journal of Antimicrobial Chemotherapy*, 69(4):881–891. 7, 63, 64, 79, 80

Steiner, C., Barrett, M., and L, T. (2012). HCUP projections: *Clostridium difficile* hospitalizations 2011 to 2012. *HCUP Projections Report # 2012-01*. 61, 62

Talpaert, M. J., Gopal Rao, G., Cooper, B. S., and Wade, P. (2011). Impact of guidelines and enhanced antibiotic stewardship on reducing broad-spectrum antibiotic usage and its effect on incidence of *Clostridium difficile* infection. *Journal of Antimicrobial Chemotherapy*, 66(9):2168–2174. 7, 63, 64, 65

Tilman, D. and Kareiva, P. (1997). *Spatial Ecology: The Role of Space in Population Dynamics and Interspecific Interactions*. Monographs in population biology. Princeton University Press. 8

U.S. Department of Health and Human Services (2013). National action plan to prevent health care-associated infections: Road map to elimination. Technical report. 61

Webb, G., Blaser, M. J., Zhu, H., Ardal, S., and Wu, J. (2004). Critical role of nosocomial transmission in the toronto sars outbreak. *Mathematical Biosciences and Engineering*, 1(1):1–13. 62

Yahdi, M., Abdelmageed, S., Lowden, J., and Tannenbaum, L. (2012). Vancomycin-resistent enterococci colonization-infection model: parameter impacts and outbreak risks. *Journal of Biological Dynamics*, 6(2):645. 62

Vita

Jason Loran Bintz was born in Memphis, Tennessee in 1974. He graduated from Knoxville Catholic High School in 1993 and received a Bachelor of Arts in Mathematics from Covenant College in 2003. While teaching high school mathematics in Chattanooga, Tennessee, he met and married Claire Catching who was also a teacher. In 2005, they moved to South Hamilton, Massachusetts where Jason studied theology and received a Master of Divinity while Claire continued her service in public education. After a brief stop teaching high school mathematics again, Jason and Claire moved to Knoxville where he began graduate studies in mathematics at the University of Tennessee. During this time, Claire completed a Master of Education with a special emphasis in autism and gave birth to their three children, Jon Loran (4), Evelyn Claire (2), and Stephen Cole (8 mo.).

Their next stop is in Houghton, New York where Jason will be Assistant Professor of Applied Mathematics at Houghton College.